27. SEDIMENTOLOGY

A.O. Beall, Jr., Continental Oil Company, Ponca City, Oklahoma,
R. Laury, Department of Geology, Southern Methodist University, Dallas, Texas,
K. Dickinson, U.S. Geological Survey, Corpus Christi, Texas,
and
W.C. Pusey, III, Continental Oil Company, Ponca City, Oklahoma

MAJOR SEDIMENT TYPES

Deep-water sediments recovered from Leg 10 of the Deep Sea Drilling Project in the Gulf of Mexico (Figure 1) comprise a spectrum between biogenically dominated pelagic sediments and terrigenous clastics, usually characterized as laminites and turbidites (Beall and Fischer, 1969). In the southern Gulf of Mexico, both shallow and deep-water carbonates comprise important lithologies. This chapter will attempt to review the sedimentological attributes of sediments recovered on Leg 10 by discussing observations made during core description, smear slide study, coarse fraction study, X-ray analysis, textural analysis, carbon-carbonate analysis, limited petrographic study of thin sections (primarily of carbonates and cherts), and a review of physical properties. Sediments recovered can be categorized as follows:

- Organogenic pelagic sediments.
  - Nannoplankton oozes and chalks.
  - Volcanic ash deposits and bentonites.
  - Minor radiolarian cherts.
- Abyssal plain terrigenous turbidites and laminites.
  - Sand- and silt-dominated turbidites.
  - Clay- and mud-dominated laminites.
- Shallow-water carbonates.
  - Limestones.
  - Dolomites.
- Deep-water limestones.
  - Calcilutites and calcarenites.
  - Pebbly mudstones.

Descriptions of deep-water pelagites, laminites, and turbidites from the Gulf of Mexico were treated at length by Beall and Fischer (1969) and will not be repeated here; sediments of these types recovered during Leg 10 coring were quite similar in all respects. In order to reduce repetition and still cover pertinent data, discussion of sediment types will proceed without a conventional discussion of each sediment type followed by textural data, mineralogical data, and so on. Under the heading of "Textural Composition of Sediments," for example, sedimentary structures and general composition will be discussed in relation to examples cited. The only departure from this format will be under the topics of deep-water limestones, shallow-water carbonates, and cherts, which by nature of their less common occurrence have received special attention, primarily in terms of petrographic study.

TEXTURAL COMPOSITION OF SEDIMENTS

Conventional sand-silt-clay analyses were performed on each core section, where possible, by Deep Sea Drilling Project shore-based laboratories (this report), with subsidiary detailed sieve analyses carried out by Beall. In addition, observations by shipboard scientific staff while preparing visual core descriptions have greatly enlarged the data base. Broader interpretations are made possible by incorporating all data.

Percentages of sand, silt, and clay are summarized in Figure 2 for all sites. Samples were preferentially taken from the most representative lithologies, which are most often the finest grained. It should be pointed out that analyses performed on semi-consolidated ooze or disturbed chalk are undoubtedly biased in that percentages of sand and silt are probably higher than in the original textural mix. Nevertheless, valuable information can be deduced from the aforementioned plot.

For purposes of discussion, the above defined textural data can be displayed (Figure 2) under four main categories: (1) abyssal plain sediments, (2) continental rise sediments, (3) carbonate slope sediments, and (4) sediments which accumulated on salt structures, primarily pelagic in terms of dominant sedimentary composition. The last category is somewhat arbitrary and was selected to explain some important differences which exist between such sediments and other depositional settings.

On a sand-silt-clay basis, abyssal plain sediments exhibit a skewed distribution of sediment composition (Figure 2). The clays and muds are typically sand poor, as well as exhibiting other characteristics to be discussed later. By comparing abyssal plain sediments with carbonate slope muds and pelagic sediments capping salt dome structures, a clear indication of textural separation is displayed. The "high" sand content of the pelagic sediments is due to the presence of abundant planktonic foraminifera tests.

Continental rise sediments are typically finer grained than abyssal plain sediments, according to Figure 2. This primarily reflects the lack of coarser-grained "turbidites" at rise positions sampled. Also note that finer-grained rise and abyssal plain sediments are quite comparable in terms of proportions of silt and clay, a prime reflection of their common terrigenous source.

Pelagic sediments accumulating on the crests of salt structures are apparently finer grained than their slope counterparts. Although not supported by detailed study, it appears likely that higher biogenic productivity on the continental slope (off Yucatan), as compared to the bathymetrically more remote salt structure sites, may have resulted in a coarser-grained sediment where planktonic foraminifera, of silt-and sand-size tests, make up a dominant component.

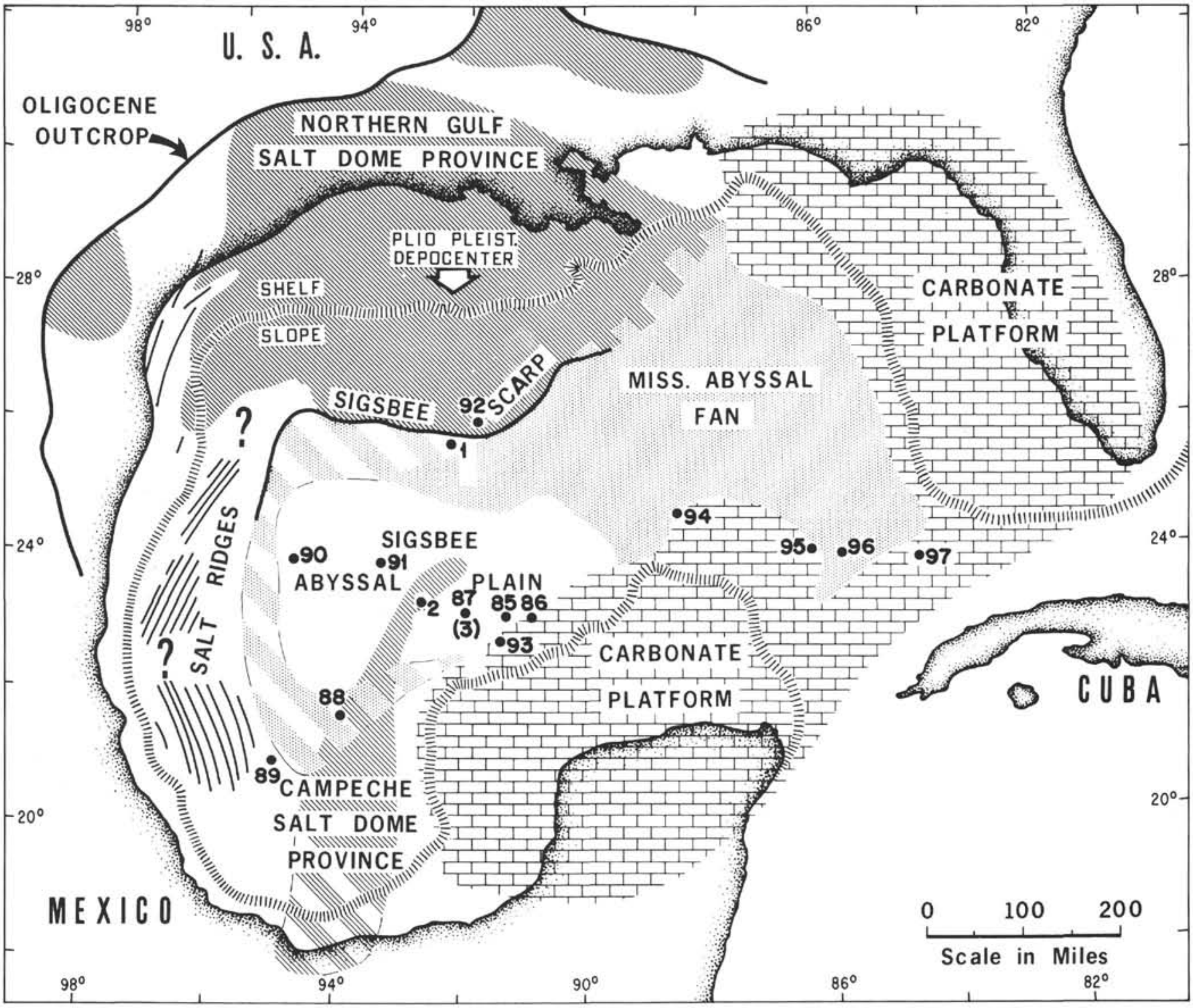

Figure 1. *DSDP Leg 10 drill sites in the Gulf of Mexico.*

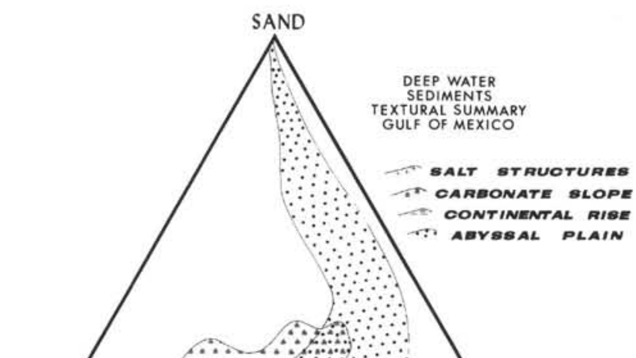

Figure 2. *Sand-silt-clay percentages.*

In addition to discrimination on the basis of carbonate versus clay mineral composition, detailed investigations have shown that the abyssal plain muds and clays are typically enriched in terrigenous organic debris. X-ray analysis typically shows enrichment of illite and kaolinite in such sediments, whereas pelagites are relatively enriched in montmorillonite. This mineralogical differentiation is thought to reflect the textural composition of the laminites (being coarser-grained and terrigenous silt-rich) as contrasted with that of the pelagites (representing pelagic outfall).

Abyssal plain turbidites, of prime interest to sedimentologists, are quite variable in textural composition. Although the term *turbidite* is often restricted to sand units, the writers accept a broader definition which encompasses finer textural grades. Turbidites of the Gulf of Mexico abyssal plain can be described as poorly to very poorly sorted silts, sandy silts, silty sands, sands, and slightly gravelly to gravelly sands. One sample of very coarse, sandy gravel has been described from Site 91. It should be pointed out that only "undisturbed" samples were used for detailed textural investigation.

Figure 3 shows a plot of median grain-size versus per cent less than 0.062 mm. (total silt plus clay fraction), as determined by wet sieve analysis. These analyses, reported in Table 1, are the result of onshore laboratory studies by Beall. All of the samples shown in the plot possess the attributes of turbidites, as defined by textural grading, sharp lower contacts, and sedimentary structures (Beall and Fischer, 1969). The plot clearly indicates the spectrum of variability involved. The enclosed area labeled "sand," which contains those samples with less than 10 per cent silt plus clay, does not exhibit clear trends of per cent "matrix" versus median. It can be noted, however, that no samples had less than 3 per cent "matrix." This can be contrasted with shallow-water sediments, and especially strandline sands, where fine sands with 3 per cent silt plus clay are somewhat less common (Beall, 1970).

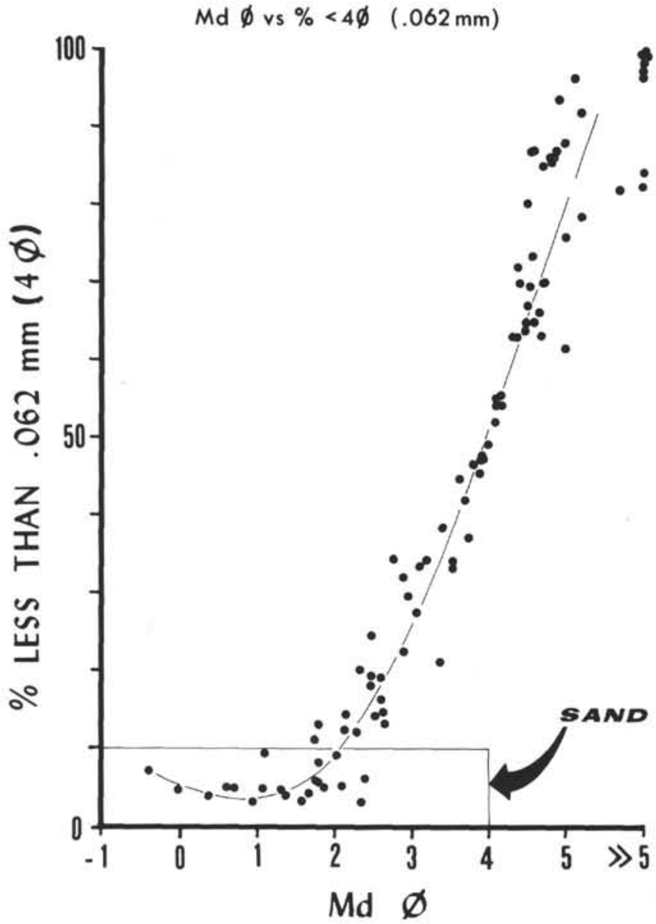

Figure 3. *Median grain-size versus percent silt-clay fraction from selected samples.*

Several examples of turbidite sequences have been selected for detailed discussion. Beall and Fischer (1969, p. 541-542 and 565-570) previously presented results of a detailed investigation of an Upper Pleistocene turbidite from the Gulf of Mexico, which exhibited more or less ideal textural grading. That investigation showed that grading was exhibited on the basis of median grain size as well as on the basis of per cent fine fraction. Maximum grain size also generally reflected the decrease of size upwards, especially in the abundance of woody debris near the top of the unit.

Figure 4 shows a somewhat more complex case of textural grading also from Upper Pleistocene sediments (Site 91). Note that sandy coarse silt, with a median of 4.15 ϕ, is the coarsest sediment contained in the sequence. Approximately 2 meters thick, the overall aspect is a fining upwards sequence. In detail, there is a suggestion of at least two graded units superimposed. The presence of two coarser units with apparent massive bedding overlain in turn by horizontally laminated units supports the interpretation of at least two genetic units. The upper cross-laminated sequence may also be a complex of yet another graded interval. The unconsolidated nature of the core makes further interpretation difficult. The coarse fractions of all samples from this sequence were dominated by organic carbonaceous debris, becoming relatively more abundant upwards as might be expected.

Figure 5 shows two examples of coarse-grained sequences of Miocene age, one from Site 87 and the other from Site 90. Although plots of textural parameters appear erratic, utilization of sedimentary structures as well as textural composition facilitates interpretation of the data. Both sequences apparently contain superimposed graded units. The absence of fine-grained tops is suggestive of erosion prior to deposition. Note that the upper graded unit of the example from Site 90 appears to be reversely graded, with the maximum grain size occurring approxiamtely 20 cm above the base.

In summary, the textural data cited above supports the following conclusions:

1) Large thicknesses of sediments with characteristic textural compositions and sedimentary structures corresponding to the concept of turbidites are common in the Gulf of Mexico Abyssal Plain.

2) Enlargement of the concept of turbidites to include a spectrum of textural grades extending into the silt grades (and possibly finer) appears necessary. The association of these sediment types and their location of several hundred miles from known shelf edges in the Gulf of Mexico argue for transport by high energy, turbid sediment masses. Thinning of stratigraphic intervals from the modern shelf edge towards the center of the abyssal plain supports such an interpretation.

3) The presence of gravelly, medium grade sands within the Miocene sequence in the center of the abyssal plain was initially surprising. Depositional rates of such sediments are quite comparable to the high depositional rates of Upper Pleistocene sediments from the same locale. With no indication of significant changes in depth of water since Miocene time, it is concluded that grain size is more closely related to provenance than to distance from provenance. Mineralogical evidence, discussed later, supports differences in provenance for the two intervals under discussion. It might be further suggested that eustatic changes in sea level during Miocene time within the Gulf

TABLE 1A
Sieve Analyses, DSDP Leg 10

	Per Cent Coarser than												
Sample	-1.0ϕ	0.28ϕ	1.25ϕ	2.0ϕ	2.52ϕ	2.75ϕ	3.0ϕ	3.25ϕ	3.75ϕ	4.5ϕ	MD ϕ	% Finer Than 4ϕ	Textural Classification (Folk)
91-1-2(105-107)	–	–	–	–	–	–	–	–	0.07	0.14	Hi	99.91	?
91-1-2(119-121)	–	–	–	–	–	–	–	–	0.22	0.66	Hi	99.35	?
91-1-2(130-133)	–	–	Tr	0.08	0.16	0.38	0.69	0.92	1.68	4.66	Hi	97.35	?
91-1-2(145-147)	–	–	–	Tr	Tr	Tr	0.08	0.16	0.42	1.84	Hi	99.25	?
91-1-3(5-7)	–	Tr	Tr	0.06	0.12	0.30	0.48	0.71	1.86	11.33	>>5 ?	96.5	Silt
91-1-3(26-28)	–	0.07	0.21	0.69	0.96	1.17	1.38	1.93	4.68	20.43	~5.2	92.0	Silt
91-1-3(42-44)	–	–	Tr	0.06	0.12	0.18	0.39	1.12	7.59	34.63	~4.8	85.5	Sdy crse silt
91-1-3(60-62)	–	Tr	0.10	0.57	1.50	4.40	7.86	17.74	35.11	51.86	4.15	55.5	Sdy crse silt
91-1-3(83-85)	–	–	Tr	0.07	0.14	0.21	0.42	1.20	6.14	29.86	~4.98	88.0	Sdy crse silt
91-1-3(100-102)	–	–	Tr	Tr	0.07	0.14	0.26	0.86	6.12	31.53	~4.88	87.0	Sdy crse silt
91-1-3(115-117)	–	0.07	0.26	0.52	0.78	1.24	1.95	5.14	15.69	33.33	~5.2 ?	78.5	Sdy silt
91-1-3(130-132)	–	0.07	0.42	1.11	1.52	2.15	2.70	4.99	12.68	28.83	~5.7 ?	82.0	Sdy silt
91-1-3(143-145)	–	–	Tr	Tr	0.27	1.98	3.85	8.96	22.65	49.42	4.52	69.5	Sdy crse silt
91-1-6(79-82)	–	–	–	Tr	0.07	0.14	0.21	0.28	0.54	4.05	~6 ?	99.0	Silt
91-1-6(91-94)	–	–	–	Tr	Tr	0.05	0.10	0.25	2.42	24.70	~4.9	93.5	Crse silt
91-2-4(114-116)	–	–	–	–	–	–	–	–	Tr	0.06	V. Hi	99.98	Clay ?
91-2-4(130-133)	–	Tr	Tr	0.05	0.15	0.35	0.45	0.50	0.76	1.48	Hi	99.05	Mud ?
91-2-4(145-147)	–	–	–	Tr	Tr	Tr	0.05	0.15	0.83	5.31	~6.0	98.3	Silt
91-2-5(8-10.5)	–	–	Tr	0.07	0.14	0.21	0.28	0.42	1.34	18.24	~5.1	96.4	Silt
91-3-6(90-92)	–	–	–	–	–	–	–	–	–	0.26	Hi	V. Hi	Clay/Mud ?
91-4-6(103-105.5)	–	–	–	–	–	–	–	–	–	Tr	V. Hi	~100	Clay/Mud?
91-4-6(112-114.5)	–	–	–	–	–	–	–	–	–	0.07	V. Hi	99.99	Clay/Mud ?
91-4-6(124.5-127)	–	Tr	0.05	0.10	0.15	0.30	0.35	0.50	0.60	2.93	~6.5 ?	99.1	Silt ?
91-7-1(75-77.5)	–	Tr	0.05	0.10	0.45	1.02	1.56	3.07	10.18	50.54	4.48	80.0	Sdy crse silt
91-7-1(96-98.5)	–	Tr	0.04	0.08	0.27	0.45	0.54	1.17	5.84	45.76	4.58	87.0	Sdy crse silt
91-7-1(112-114.5)	Tr	Tr	Tr	0.05	0.25	0.54	0.94	1.92	5.86	46.28	4.55	87.0	Sdy crse silt
91-7-1(130-132.5)	–	Tr	0.05	0.15	0.48	1.07	1.66	3.49	8.54	33.40	4.85	86.0	Sdy crse silt
91-7-1(143-145.5)	–	Tr	0.05	0.10	0.39	0.87	1.35	2.89	8.10	39.07	4.70	85.0	Sdy crse silt
91-7-2(34-36)	0.05	0.10	0.22	0.49	1.09	2.39	3.74	6.89	16.33	56.92	4.37	72.0	Sdy crse silt
91-7-2(57.5-60)	Tr	Tr	0.15	0.54	1.23	2.85	3.83	8.30	27.01	56.48	4.30	63.0	Sdy crse silt
91-7-2(73-75.5)	Tr	0.12	0.68	1.23	1.97	2.83	3.44	5.84	27.68	56.03	4.35	63.0	Sdy crse silt
91-7-2(91.5-94)	–	Tr	0.13	0.50	1.19	2.51	3.70	7.02	19.12	54.61	4.40	70.0	Sdy crse silt
91-7-2(111.5-114)	–	Tr	0.05	0.10	0.88	2.79	4.93	9.47	20.53	44.77	4.70	70.0	Sdy crse silt
91-7-2(128.5-131)	–	Tr	Tr	0.07	0.11	2.77	4.94	10.82	22.92	49.0	4.50	67.0	Sdy crse silt
91-7-2(141-143.5)	Tr	0.07	0.21	0.60	1.20	3.22	5.92	13.93	35.66	67.34	4.1	54.0	Sdy crse silt
91-7-3(15-17.5)	–	Tr	0.07	0.14	2.26	8.08	13.84	26.15	50.25	79.53	3.73	37.0	Silty, v.f. sd
91-7-3(35.5-38)	–	–	Tr	0.06	0.68	3.65	7.11	14.71	35.78	71.08	4.08	52.0	Sdy crse silt
91-7-3(52.5-55)	–	0.06	0.09	0.12	1.07	4.26	7.15	17.14	40.07	68.38	3.98	49.0	Silty, v.f. sd
91-9-4(40.5-54)	–	Tr	0.29	2.26	6.49	14.59	23.27	37.56	58.50	75.20	3.52	34.0	Silty, v.f. sd
91-9-4(53-55.5)	–	0.17	0.68	2.20	5.91	12.75	19.43	33.87	52.20	64.27	3.69	42.0	Silty, v.f. sd
91-9-5(73-75.5)	–	–	0.60	1.80	3.06	5.51	8.51	17.38	37.03	60.52	4.15	54.0	Sdy crse silt
91-9-5(81-83.5)	–	–	0.59	0.89	2.18	9.39	14.17	35.36	60.21	74.91	3.53	33.0	Silty, v.f. sd
91-9-5(89.5-92)	–	–	0.12	0.29	0.40	0.98	2.76	12.65	41.29	71.31	3.92	47.0	Silty, v.f. sd
91-9-6(8-11)	–	Tr	0.11	0.44	1.00	3.21	5.92	14.12	30.90	47.90	4.68	63.0	Sdy crse silt
91-9-6(17-19.5)	–	–	–	–	Tr	0.05	0.20	1.02	6.62	37.08	4.8	86.0	Sdy crse silt
91-9-6(33-36)	–	–	0.55	0.82	1.99	5.48	10.42	23.24	44.69	64.91	3.90	47.0	Silty, v.f. sd
91-9-6(48-50.5)	–	Tr	0.57	0.86	1.85	5.71	10.70	21.47	44.94	64.05	3.90	47.0	Silty, v.f. sd
91-9-6(59-61.5)	–	0.06	0.42	0.66	1.20	3.60	7.73	17.81	37.17	60.55	4.12	55.0	Sdy crse silt
91-18-6(130-132)	0.53	4.78	14.65	28.77	40.68	46.97	51.17	56.44	64.18	73.44	2.90	32.0	Silty, find sd
91-18-6(147-149)	0.05	1.52	8.18	19.76	29.67	35.57	39.04	44.18	51.92	61.61	3.61	44.5	Silty, v.f. sd, sli. gravelly

91-20-2(33-36)	0.08	0.70	4.64	17.09	40.99	58.70	66.74	76.72	83.53	87.47	2.63	14.5	Silty, fine sd
91-20-2(140-142)	–	1.87	9.70	23.14	49.71	68.13	70.65	77.25	84.62	87.72	2.52	14.0	Silty, fine sd
91-20-6(46-48)	0.84	2.86	13.18	25.80	44.07	58.58	65.55	73.78	81.45	86.47	2.60	16.2	Silty, fine sd
91-20-6(133-135)	0.48	2.68	10.26	22.30	43.83	61.30	64.22	70.72	78.47	83.36	2.60	19.0	Silty, fine sd, sli. gravelly
91-22-1(81-83.5)	–	0.12	16.41	60.65	79.92	85.04	86.73	89.29	91.50	92.9	1.81	8.0	Med. sd, sli. gravelly
91-25-1(94-96)	–	0.06	2.23	22.77	59.15	76.0	81.47	88.62	93.14	95.2	2.39	5.9	Fine sd
91-25-1(100-102)	–	0.07	9.81	39.42	76.38	88.14	89.52	92.37	94.35	95.33	2.13	5.1	Fine sd
91-25-1(140-142)	–	Tr	7.21	43.37	75.00	85.48	89.33	92.40	94.71	95.82	2.10	4.9	Fine sd
91-25-2(60-62)	–	0.90	29.99	66.53	84.82	90.43	92.41	93.92	95.24	96.18	1.65	4.1	Medium sd
91-25-2(128-131)	–	3.45	42.88	77.42	89.93	93.05	94.22	95.11	95.77	96.61	1.39	3.8	Medium sd
91-25-3(67-69)	0.05	20.01	64.06	88.30	93.93	95.09	95.34	95.87	96.55	97.13	0.95	3.1	Sli. gravelly, crse sd
91-25-3(102-104)	0.59	31.46	70.42	88.40	92.40	93.33	93.68	94.27	94.96	95.80	0.70	4.8	Sli. gravelly, crse sd
91-25-3(132-134)	2.79	36.81	71.13	88.72	91.55	92.54	92.96	93.87	94.89	95.88	0.60	4.9	Sli. gravelly, crse sd
91-25-4(10-11)	12.67	45.61	82.19	91.78	93.44	94.06	94.46	95.26	95.95	96.92	0.38	3.9	Gravelly crse sd
91-25-4(24-25)	19.75	59.37	86.89	91.62	92.94	93.84	94.02	94.97	96.35	96.95	−0.03	4.4	Gravelly, v. crse sd
91-25-4(41-42)	31.89	65.62	76.76	81.01	84.68	86.80	87.61	88.59	92.45	94.79	−0.41	7.0	V. crse sdy gravel
91-25-4(60-62)	0.55	1.38	4.13	18.73	40.01	56.82	64.05	75.00	84.78	90.36	2.65	12.9	Sli. gravelly, silty fine sd
91-25-4(64-66)	–	0.14	0.86	5.09	9.31	14.90	22.92	42.41	71.99	87.25	3.37	21.0	Silty, v.f. sd
91-25-4(98-100)	0.05	4.01	19.88	60.28	81.08	87.84	90.30	93.00	94.84	95.99	1.84	4.7	Sli. gravelly, med. sd
91-25-4(108-110)	0.81	4.27	18.84	62.25	80.87	86.75	88.89	91.61	93.97	95.22	1.80	5.5	Sli. gravelly, med. sd
91-25-4(129-130)	0.13	1.57	45.95	83.09	90.45	92.46	93.09	94.22	95.16	96.04	1.31	4.4	Sli. gravelly, med. sd
85-2-1(124-126.5)	–	0.07	0.65	2.98	5.81	8.21	9.95	12.27	15.83	21.28	>>5	82.5	Sdy silt (?)
85-2-1(136-138.5)	–	Tr	1.71	8.71	15.93	20.85	23.45	28.29	35.15	44.53	~5	61.5	Sdy silt
85-2-1(146.5-149)	–	0.07	4.82	25.20	40.18	46.97	50.91	56.25	64.13	73.78	2.90	32.0	Silty, fine sd
85-2-2(4-6.5)	–	0.12	1.86	12.11	23.66	29.88	34.10	39.88	49.32	61.37	3.81	46.5	Silty, v.f. sd
85-2-2(13-15.5)	–	2.2	9.97	37.35	54.89	62.12	65.60	70.41	76.91	84.20	2.32	20.0	Silty, fine sd
85-5-1(125-127)	–	0.05	0.92	17.84	68.44	87.06	91.97	95.23	96.74	97.66	2.35	2.9	Fine sd
85-5-2(125-127)	0.36	7.25	35.60	71.50	88.34	93.26	94.87	96.32	96.89	97.36	1.59	3.0	Sli. gravelly, med. sd
87-1-2(75-76)	–	0.09	1.77	5.22	8.50	10.53	11.42	13.10	14.96	17.52	>>5	84.2	Sdy silt (?)
87-1-2(79.5-82)	0.09	0.33	7.38	32.14	50.42	57.75	61.61	66.64	72.93	79.51	2.47	24.5	Sli. gravelly, silty fine sd
87-1-2(85-87.5)	–	0.06	0.96	3.04	7.22	12.54	16.84	25.73	45.73	72.78	3.89	45.5	Silty, v.f. sd
87-1-2(95-97.5)	–	1.12	7.21	22.60	36.19	44.57	49.78	56.32	66.05	77.74	2.96	29.5	Silty, fine sd
87-1-2(105-107.5)	0.04	1.02	6.57	20.39	33.72	42.03	46.56	53.31	62.99	73.83	3.1	33.5	Sli. gravelly, silty v.f. sd
87-1-2(111.5-112.5)	–	0.17	0.51	2.92	3.95	5.15	5.49	8.58	18.18	48.20	4.55	73.5	Sdy, crse silt
87-1-2(114-116.5)	–	0.26	6.48	23.37	37.64	46.99	52.06	60.01	72.14	85.31	2.90	22.5	Silty, fine sd
87-1-2(122-124.5)	–	0.13	1.58	13.11	29.26	40.53	47.12	56.67	67.70	80.75	3.05	27.5	Silty, v.f. sd
87-1-2(133-135)	–	0.13	1.22	4.50	8.99	12.27	14.58	18.75	28.90	51.25	4.48	64.0	Sdy crse silt
87-1-2(142.5-145)	0.16	2.52	7.95	18.67	28.49	34.98	39.37	46.10	56.17	70.86	3.43	38.5	Sli. gravelly, silty v.f. sd
87-1(CC)	0.10	1.76	7.87	21.11	34.34	42.17	46.29	52.05	61.93	72.19	3.18	34	Sli. gravelly, silty v.f. sd
90-10-1(46-49)	–	–	0.05	0.60	2.26	4.61	6.57	11.93	27.52	51.23	4.47	64	Sdy, crse silt
90-10-4	–	0.04	0.30	1.32	3.72	6.77	9.07	13.81	26.52	47.07	4.65	66	Sdy, crse silt
90-12(CC)	–	0.87	12.08	34.06	50.65	59.25	63.42	69.85	78.28	87.66	2.48	18	Silty, fine sd
90-13-1(51-53)	0.13	2.00	12.59	30.25	43.90	49.97	53.30	57.43	63.16	69.89	2.76	34.5	Sli. gravelly, silty fine sd
90-13-3(91-93)	–	9.06	35.98	56.13	67.21	72.75	76.21	80.77	86.70	92.44	1.75	11.0	Silty, med. sd
90-13-3(111-113)	1.25	30.43	52.88	67.45	75.71	80.00	82.50	85.71	89.18	92.92	1.10	9.2	Sli. gravelly, med. sd
90-13-3(129-131)	0.29	10.98	34.78	55.00	65.63	71.46	74.64	79.15	84.46	90.06	1.80	13.0	Sli. gravelly, med. sd
90-13-3(145-147)	–	1.08	17.50	44.25	58.42	66.74	72.00	78.25	85.17	91.75	2.28	12.0	Silty, fine sd
90-13-4(11-12)	–	1.18	21.41	46.15	60.28	67.45	71.63	77.19	84.69	91.11	2.12	12.7	Silty, fine sd
90-13-4(35-40)	–	3.06	24.66	46.20	58.87	65.87	70.12	76.01	82.79	88.97	2.13	14.5	Silty, fine sd
90-13-4(51-52)	0.12	8.71	33.48	59.05	72.81	80.58	84.38	88.36	92.66	96.45	1.73	5.8	Sli. gravelly, med. sd
90-13-4(57-58)	–	3.14	25.89	49.39	64.01	71.72	75.24	80.98	88.40	94.76	2.02	9.0	Fine sd
90-13-4(82-84)	Tr	4.85	16.97	36.72	50.23	58.03	62.88	68.71	77.08	85.62	2.48	19.5	Silty, fine sd
90-13-4(108-109)	0.65	10.13	57.65	78.46	85.00	87.94	89.32	91.39	94.01	97.28	1.08	4.8	Sli. gravelly, med. sd
96-1-6(135.5-138)	–	Tr	0.17	0.67	1.57	3.20	5.00	9.55	19.20	36.61	~5.0	76.0	Sdy crse silt
96-1-6(139-141)	–	–	0.10	0.45	2.03	5.20	8.52	15.51	28.84	47.97	4.58	65.0	Sdy, crse silt

TABLE 1B
Sieve Analysis, DSDP Leg 1

Sample	Per Cent Coarser than 1.25φ	2.75φ	3.0φ	3.25φ	3.75φ	4.5φ	Mdφ	% Finer Than 4φ	Textural Classification
1-5-2(93-94)	–	0.13	0.18	0.32	0.69	8.6	~5.2	98.8	Silt
3-2-1(73-74)	–	–	–	–	–	Tr	V. Hi	~100.0	Clay
3-2-1(83-84)	–	–	–	–	0.37	0.48	Hi	99.6	Mud
3-2-1(93-94)	0.04	0.86	1.28	1.94	4.61	23.8	5.1	91.5	Silt
3-2-1(102-103)	0.14	15.2	23.4	26.65	35.05	46.1	4.72	61.0	Sandy silt
3-2-1(113-114)	0.27	1.81	2.8	6.72	28.75	68.2	4.12	57.0	Sandy silt
3-2-1(123-124)	0.05	3.73	7.11	17.16	44.0	74.6	3.87	44.0	Silty, v.f. sd
3-2-1(133-134)	0.017	16.85	28.4	43.9	64.1	81.8	3.39	29.5	Silty, v.f. sd
3-2-1(143-144)	0.01	30.8	41.7	53.7	68.5	82.0	3.17	26.0	Silty, v.f. sd
3-2-2(3-4)	0.03	42.15	50.55	60.0	73.2	86.3	2.98	21.0	Silty, v.f. sd
3-2-2(12-14)	0.09	37.45	46.05	56.1	70.6	83.8	3.06	24.0	Silty, v.f. sd
3-2-2(23-24)	0.16	39.4	46.8	56.2	70.0	82.1	3.06	25.5	Silty, v.f. sd
3-2-2(33-34)	0.38	23.0	29.0	37.6	52.6	68.0	3.66	41.5	Silty, v.f. sd

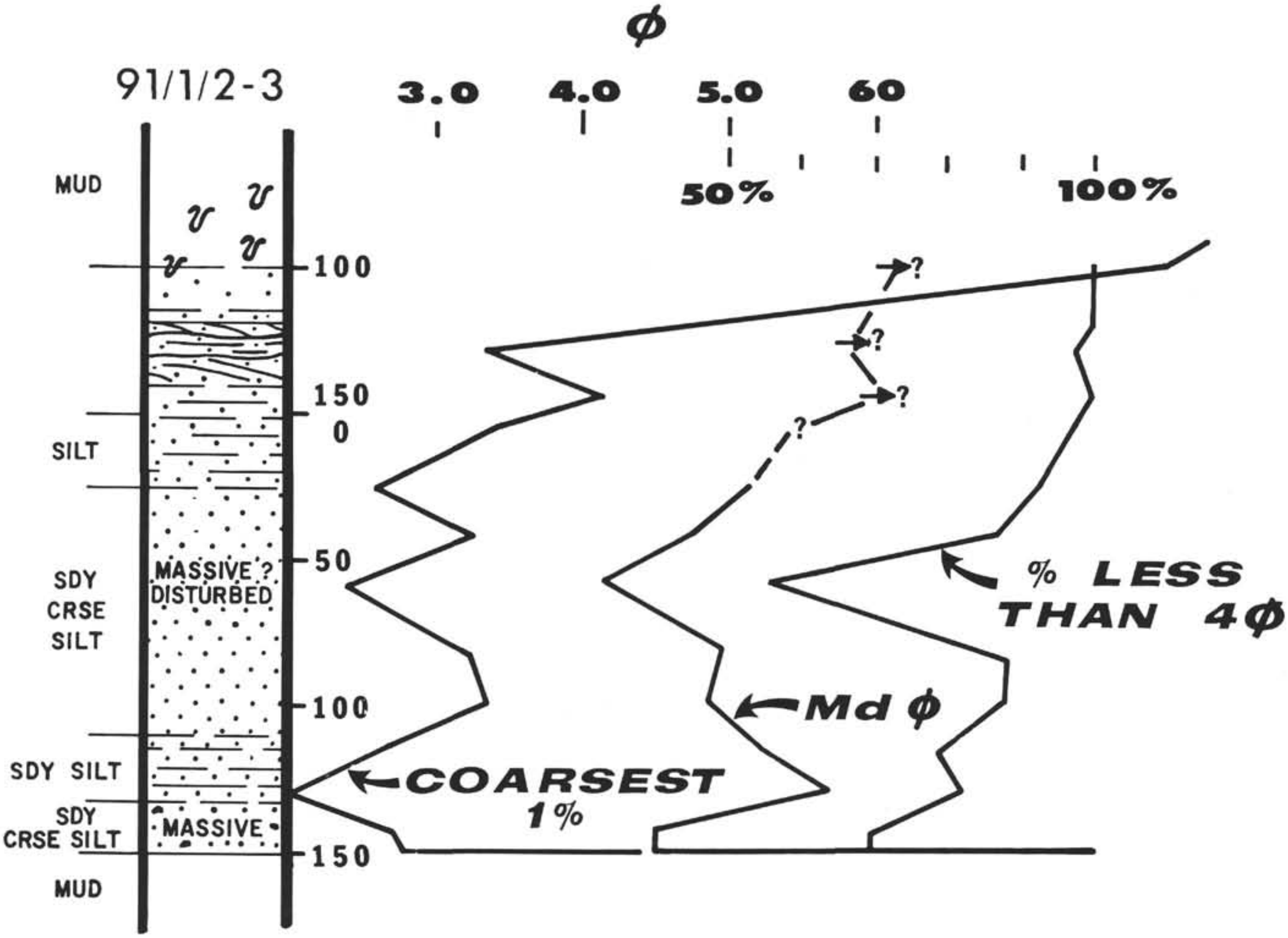

Figure 4. *Textural grading in Upper Pleistocene sediments from Hole 91.*

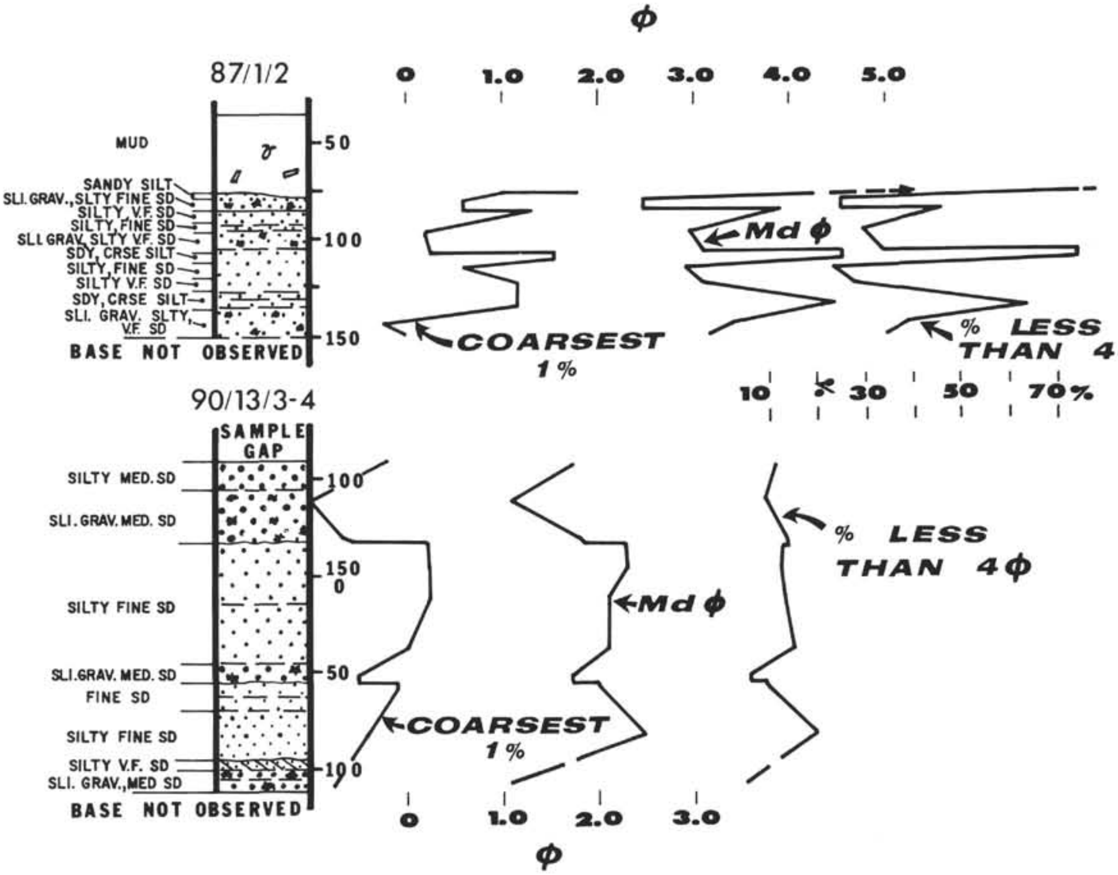

Figure 5. *Textural grading in Miocene sediments from Holes 87 and 90.*

of Mexico basin were responsible for delivering coarse-grained sediments to the then existent shelf edge where initiation of transport out onto the abyssal plain took place.

4) The presence of possible reverse grading at the base of graded beds suggests that reverse grading, as well as eroded (missing) tops of beds, is not an indicator of proximity to source. Although beyond the scope of this paper, the writers suggest that the nature of the suspension or turbidity current is responsible for such developments. It can be speculated that very high suspended sediment concentrations are responsible for the effect.

Textural data is lacking for most consolidated carbonate sediments. The limited information gained from thin section petrography will be covered in the next section, along with less common sediment types such as pebbly mudstone and cherts.

MINERALOGY AND PETROLOGY OF SEDIMENTS

The mineral composition of the sediments was determined utilizing data from (1) shipboard study of smear slides, (2) qualitative and quantitative onshore study of selected smear slides by Laury, (3) qualitative study of coarse fraction residues by Dickinson, (4) petrographic study of selected chert samples by Laury and carbonates by Pusey and Beall, (5) carbon-carbonate analyses carried out by Deep Sea Drilling Project staff, and (6) X-ray diffraction analyses. Plates 1-4 are photomicrographs of typical sediments recovered.

Common Minerals:

Mineralogically, the sediments are dominated by calcite, quartz, and clay minerals. Dolomite, and a relatively small number of common terrigenous detrital components provide most of the remaining variation in composition. X-ray diffraction data show a moderately strong inverse correlation between total carbonate content and total clay content (Figure 10). As previously discussed, pelagic sediments are strongly biased toward the high carbonate (high calcite) end of the spectrum, whereas abyssal plain sediments such as laminites and turbidites are enriched in clay minerals.

Clay mineral suites are dominated by detrital "mica," undoubtedly varying between "illite" in the finer-grained sediments and commonly biotite in the coarser-grained turbidite sands on the abyssal plain. Subsidiary clay minerals include montmorillonite, kaolinite, and chlorite in decreasing abundance. Montmorillonite appears to be more common in the northern Gulf (at Sites 92 and 91), and locally abundant in bentonitic layers at various localities throughout the area sampled. Whereas the montmorillonite has both a detrital and a volcanic source, the other clay minerals are apparently detrital in origin.

Feldspar, represented by both potassium feldspar and plagioclase, is a common constituent of most sediments dominated by terrigenous detritus. Figure 6 illustrates a ternary plot of relative percentages of quartz, potassium feldspar, and plagioclase, as determined by X-ray diffraction. For purposes of discussion, samples have been categorized as (1) Pleistocene laminites and turbidites, (2) Miocene-Pliocene laminites and turbidites, and (3) all pelagic oozes and chalks. The latter group is not represented if none of the three components was detected by X-ray diffraction. Leg I data have also been included (Rex, 1969, p. 353-357).

As shown in Figure 6, pelagic sediments tend to scatter throughout the diagram, in part a reflection of spurious small percentages of one or two components. Quartz is most common in this sediment type with quartz and plagioclase mixtures reflecting the general composition of terrigenous sediments, that is, low in potassium feldspar. Potassium feldspar is not common in any of the sediment types. Note that in some forty samples, quartz was the only mineral of the three reported.

The terrigenous-dominated sediments can be considered to represent two overlapping compositional populations. Pleistocene (and to some extent Pliocene) sediments tend to be enriched in quartz and potassium feldspar, as compared to the remaining Pliocene and Miocene laminites and turbidites, which are comparatively plagioclase rich and low in potassium feldspar. These data are taken as suggestive of two distinct terrigenous provenances, the Miocene provenance being enriched in plagioclase feldspar.

As discussed in the Site Summaries for Sites 87/3, 90, and 91, there is considerable evidence of at least two major terrigenous source areas represented by abyssal plain

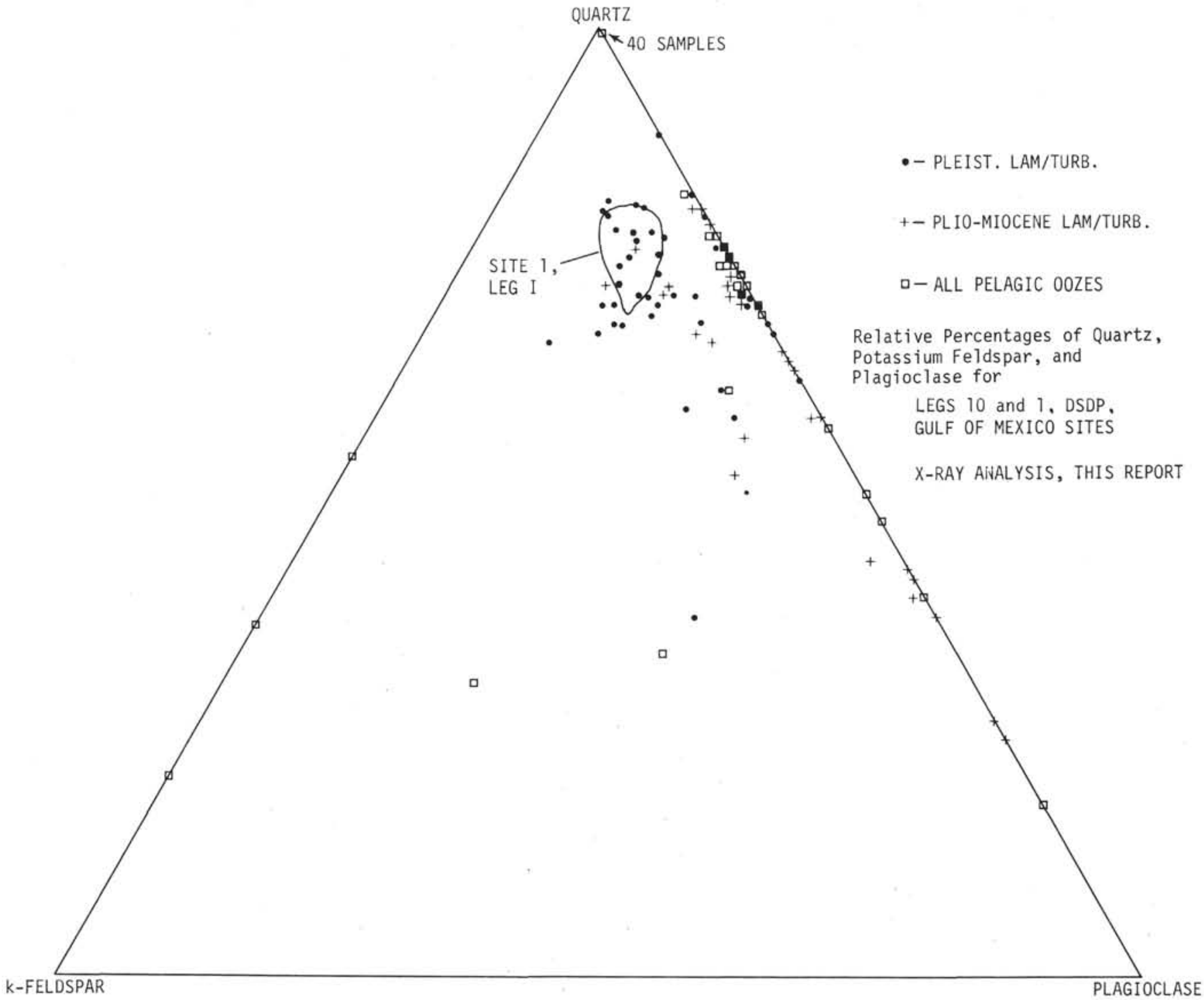

Figure 6. *Ternary plot of quartz, plagioclase feldspar, and potash feldspar as determined by x-ray.*

deposits at those locales. In addition to differentiation on the basis of feldspar and quartz, complementary mineralogical distinctions can be summarized as follows:

Pleistocene terrigenous sediments
1) High quartz content.
2) K-feldspar and plagioclase equal.
3) High montmorillonite content.
4) Common detrital dolomite.
5) Relatively mature heavy mineral suite.
6) Low carbonate and volcanic rock fragment content.

Miocene terrigenous sediments
1) Intermediate to low quartz content.
2) Enriched in plagioclase.
3) Low montmorillonite content.
4) Less common detrital dolomite.
5) Less mature heavy suite.
6) Relatively high carbonate and volcanic rock fragment content.

Figure 7 illustrates thickness relationships of the abyssal plain on a cross section from Site 90 on the western rise to a position on the abyssal plain at Site 85, near the Campeche Scarp. Easterly thinning of the Miocene section is a clear indication of contribution of detritus from the northwestern Gulf of Mexico (refer to Worzel and Bryant, this volume, for related discussions). The thick Pleistocene section, on the other hand, thickens toward the north and northeast, while thinning towards the northwest. This is taken as an indication of a primary Pleistocene source of detritus to the north and northeast.

As noted in discussions for Sites 90 and 91, there is considerable evidence, in terms of sediment color and seismic wedging, for suggesting a complex interaction of sediment contribution from the Mississippi Fan, the northern slope complex, and the northwestern (Rio Grande) slope regions (Figure 1). Although some sampling bias is undoubtedly involved, it is readily demonstrated that Pleistocene turbidites are considerably finer grained than the Miocene turbidites where both intervals have been sampled. The very coarse Miocene sands represent the coarsest-grained terrigenous detritus yet recovered from the deep-water Gulf of Mexico area.

Carbonate minerals, primarily calcite, are apparently of biogenic origin. As noted previously, pelagic components of oozes or chalks consist largely of nannofossils and planktonic foraminifera tests. Less common components are siliceous radiolarian tests, unidentifiable biogenic carbonate fragments, and trace amounts of terrigenous debris. Volcanic glass and volcanic rock fragments are locally important at most sites. Aragonite, as detected by X-ray diffraction and smear slide study, was noted in shallow cores at Sites 85, 86, 93, 94, 95, and 97. Aragonite occurrences, other than inferring disappearance with depth, are difficult to summarize.

As a product of carbon-carbonate analysis, drilling results can be summarized and interpreted in terms of two dominant trends, as shown by Figure 8. Each hole has been summarized in terms of a mean carbon versus carbonate average percentage, with the exception of Site 96, where pelagic sediments are overlain by terrigenous abyssal plain sediments. The overall mean percentages of carbon and carbonate, including Sites 1 through 3 of Leg 1, are 0.365 and 43.5 respectively. Abyssal plain sites are characteristically low in carbonate and high in carbon whereas pelagic-dominated sites are the inverse. This reflects the dominantly terrigenous source of most of the carbon, primarily from terrigenous plants, as suggested by

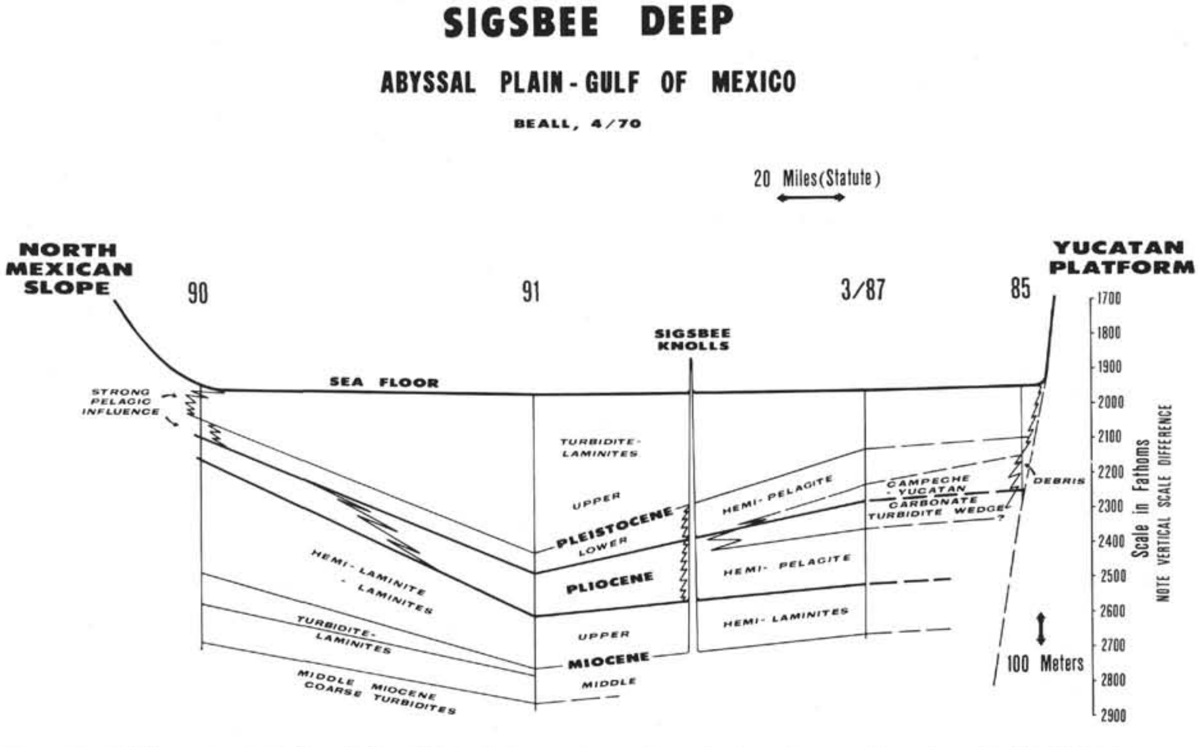

Figure 7. *Thickness and facies relationships of deepwater sediments from the southwestern Gulf of Mexico.*

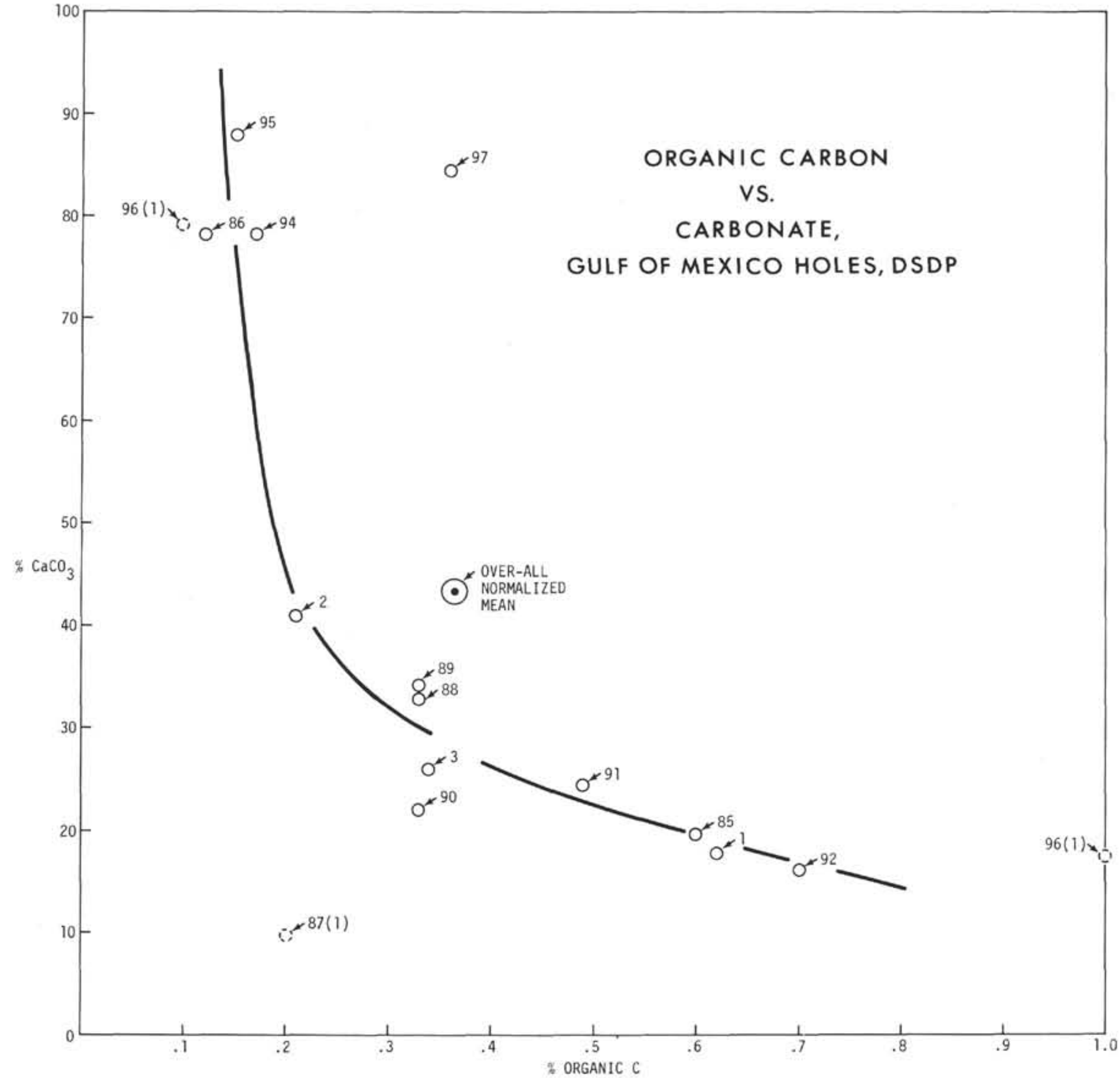

Figure 8. *Carbon-carbonate percentages.*

coarse fraction study which revealed abundant spores, carbonaceous debris, and woody fragments.

Site 97 occupies a somewhat anomalous position on the plot, an apparent result of a distinctively different depositional setting. Here the Tertiary section contains considerable terrigenous material (hemipelagic), possibly furnished in part by turbidity from the nearby abyssal plain. The underlying Cenomanian deep-water limestones are also apparently enriched in carbonaceous debris, reflecting possibly quiet, deep-water sedimentation with nearby sources of terrigenous carbon, but low amounts of terrigenous clastic detritus. These carbonates will be discussed in more detail in a subsequent section.

Less Common Mineral Occurrences

Volcanic glass and associated volcanic rock fragments are important constituents, at least locally, in most of the sites drilled. Ash is typically associated with zeolites, especially in Miocene and older sediments. Montmorillonite-rich bentonite or altered volcanic ash was infrequently encountered. The zeolite species was tentatively identified as phillipsite in smear slide description. X-ray diffraction data combines zeolites under the heading of "clinoptilolite."

Palygorskite, on the basis of X-ray diffraction data, was identified in minor amounts in Sites 85, 86, 87, 88, 89, 90, and 91. Although these occurrences are difficult to interrelate, it appears that the source of palygorskite is terrigenous and probably related to proximity to Mexico. Palygorskite was not reported in the northern Gulf of Mexico holes (Sites 1 and 92).

Lower Pleistocene sediments at Site 92 contain abundant siderite (?) occurring as well-sorted, silt-size spherulites. Although specific X-ray data are lacking, the spherulites consist of single crystals which have syntaxially overgrown a rhombic nucleus. Although similar spherulites have been found in trace amounts in almost all holes drilled on Leg 10, and a detrital origin might be referred, the large amount of siderite (?) present at Site 92 suggests authigenic or diagenetic origin. X-ray data from Site 1 of Leg 1 also show siderite in small amounts.

Heavy mineral suites, especially in the terrigenous-dominated sediments, are represented by a relatively diverse assemblage of minerals. Detrital dolomite rhombs, often with abraded morphology, are common throughout most sites. Dolomite appears to be especially common at Sites 92 and 1, and is thought to represent evidence of a northern detrital source (see discussion by Beall and Fischer, 1969).

Opaque minerals, generally pyrite, are common in most sediments studied especially in pelagic sediments. In terrigenous-dominated sediments, abundant opaque heavy minerals appear to be in large part ilmenite or possibly hematite.

Accessory heavy minerals include stable assemblages of zircon, tourmaline, and rutile. Less stable components, especially common in Miocene abyssal plain sediments, include green and brown varieties of hornblende, biotite, and chlorite aggregates (metamorphic rock fragments ?). Sphene and apatite are apparently rare. From preliminary inspection of heavy mineral assemblages, it appears that a quantitative study would be valuable in further discrimination of provenance.

Petrology of Chert from Leg 10

Chert was recovered from a number of sites on Leg 10, and ranged in age from Cenomanian (Late Cretaceous) through early Oligocene. Sites 94, 95, 96, and 97, all in the southeastern Gulf of Mexico, contained chert in association with radiolarian-rich sediments. In view of these occurrences from deep-water sedement, Laury prepared thin sections of most cherts sampled. Chert formation has, in all cases but one, taken place by late post-depositional replacement of deep-water, calcareous, foraminiferal nannoplankton ooze. At each site the degree of silicification of the carbonates appears to increase with increasing age, attaining a maximum in Eocene and Paleocene sediments. Depth of burial and/or depth of the overlying water mass appear to be unrelated to the degree of silicification.

Age and lithologic composition of the host rock appear to be the major parameters controlling the formation of chert. Based on the stratigraphic occurrence of chert recovered on other Deep Sea Drilling Project legs to date, chert is not common in rocks of less than 10 to 15 million years of age. At the other end of the scale, the youngest completely recrystallized cherts obtained on Leg 10 (that have undergone complete silicification and recrystallized to microcrystalline alpha quartz) are Late Cretaceous (Campanian) in age. Thus, once silica replacement begins, it may take tens of millions of years for complete recrystallization. These figures are in agreement with other workers in this area of study (A.G. Fischer, personal communication, 1971).

In addition to composition, it is apparent that initial effective porosity and permeability of the sediment is important in controlling the pattern of replacement. For example, in extensively bioturbated chalks, silica replacement is extremely patchy and irregular (Plate 5, Figures 2 and 3). Silica fronts tend to follow burrow zones rather than proceeding uniformly. Where sediment laminae are preserved, however, permeability is greatest parallel to stratification and silica fronts parallel those planes (Plate 5, Figures 4-6).

The source of silica need not be from within the bed in which chert is formed. Dissolution of siliceous microorganisms (radiolaria, diatoms, silicoflagellates, sponge spicules, etc.) at depth and in appreciable quantity is the apparent source of silica for most chert observed on Leg 10.

Silicification begins with the replacement of fine micritic matrix within foraminiferal tests by opaline silica. Chertification apparently proceeds in the following manner. Voids within the tests are quickly filled, either with opal-cristobalite or with fibrous, length-fast chalcedony. Opalization spreads to matrix carbonate outside the tests. Foram test walls are then replaced by chalcedony, whereas test-filling opal which has not been replaced by chalcedony becomes more ordered optically and crystallizes into a fine mosaic of alpha-cristobalite (Plate 5, Figure 1). Ultimate maturity in silicification involves conversion of all opal to cristobalite, and cristobalite to subequant, microcrystalline alpha-quartz. Fibrous chalcedony is stable and may persist in highly silicified rocks (Plate 5, Figures 4-6). Fossils may be preserved as ghosts or may be completely obliterated. Finely comminuted plant material and carbonaceous debris are apparently unaffected by silicification (Plate 5, Figures 4-6).

The increasing abundance of siliceous microorganisms and occurrence of chert within several stratigraphic horizons as drilling proceeded towards the southeastern Gulf of Mexico originally suggested that a silica gradient might be present in that region. Inasmuch as the source of the silica can be thus interpreted as biogenic and pelagic, it appears logical that entry of abundant pelagic organisms via the Yucatan and Florida straits, especially during early Tertiary time, would yield such a gradient.

Petrology of Limestones and Dolomites

Consolidated limestones and dolomites recovered on Leg 10 can be considered in two main categories: (1) shallow-water carbonates consisting of interbedded limestone and dolomite and (2) deep-water limestones, consisting of interbedded calcilutites, calcarenites, and pebbly mudstones. Pusey and Beall prepared a number of thin sections of the above named rock types in order to more clearly elucidate their composition and depositional history. Most of the following description is taken from Pusey, using the carbonate terminology of Dunham.

SHALLOW-WATER CARBONATES

Shallow-water limestones and dolomites were recovered from three sites (86, 94, and 95) on the outer Yucatan platform and slope (Fig. 1). Most of the core recovery consisted of core catcher fragments, especially at Site 86. Site 94 Core 39, however, consisted of a relatively undisturbed segment some 110 cm in length. This sequence was chosen for detailed petrographic investigation and is illustrated in Figure 9.

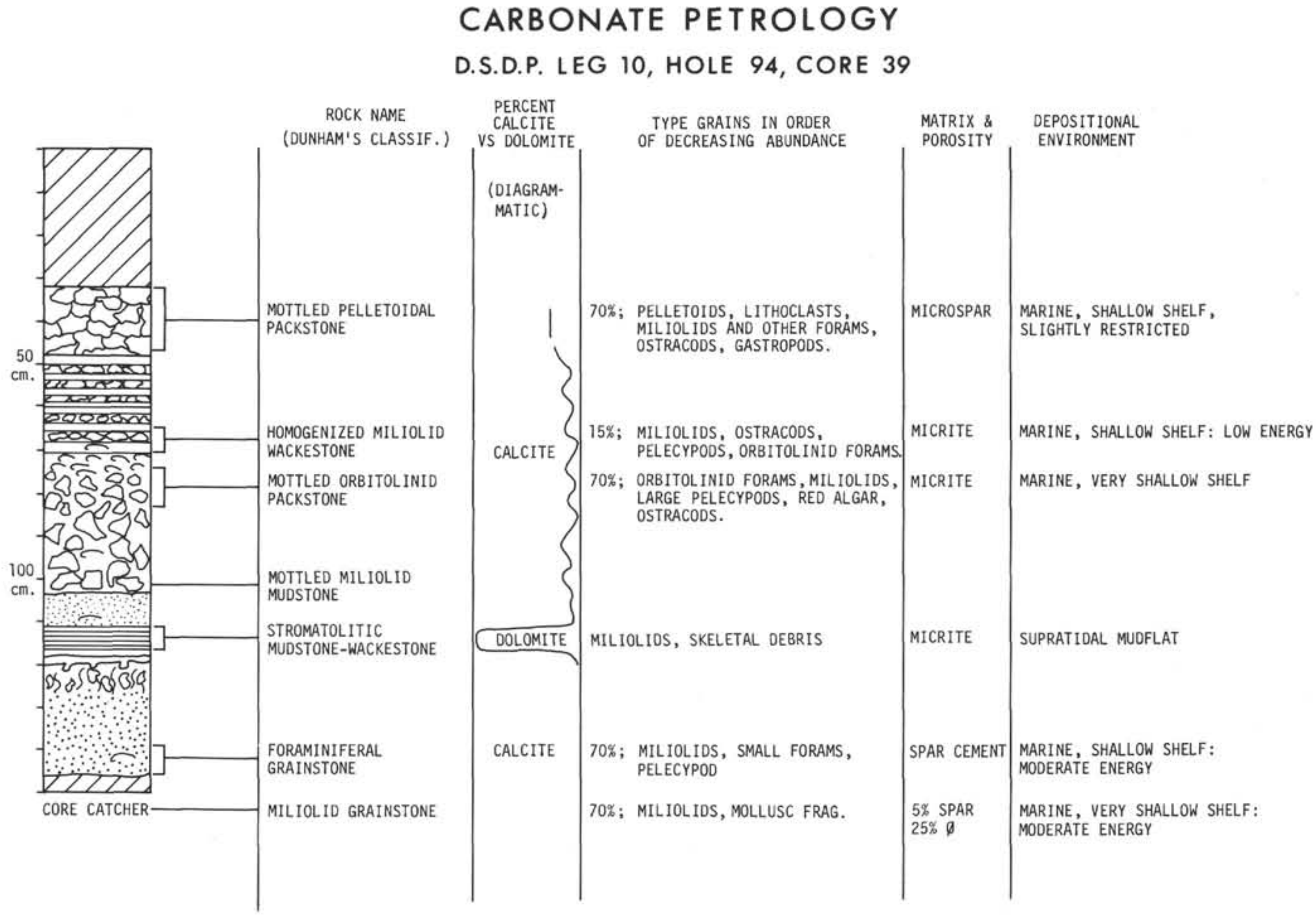

Figure 9. *Sedimentologic and petrologic interpretation of shallow-water Cretaceous carbonates from Hole 94.*

In general, the rocks consist of odorous, finely laminated lime mud overlying a highly leached section of very pale orange, slightly dolomitic grainstones, packstones, wackestones, and mudstones. Carbonate grains are characteristically miliolids, orbitolinid forams, pelecypods, gastropods, ostracods, pellets, and lithoclasts. The grainstones are characteristically selectively leached with moldic porosity and vugs lined with spar infill and dolomite. The common presence of dolomitized, algal mat-type stromatolites with preserved desiccation cracks (Plate 6), and paleontologically determined shallow-water miliolids in the carbonate sands and muds suggests a shallow-marine to supratidal environment of deposition. Pusey states further that a very shallow-marine environment is suggested by the micrite-rimmed skeletal grains, which are probably evidence of algal-fungal boring. Miliolid-rich carbonate muds and sands are characteristic of restricted shallow shelf deposits in the Lower Cretaceous (Edwards and Glen Rose formations) of Texas and northern Mexico (Behrens, 1965, Griffith et al., 1969).

More highly dolomitized rocks from these sites are generally identifiable as grainstones or wackestones. Porosities may exceed 25 per cent in some cases. The presence of a mottled to possibly brecciated fabric suggests considerable post-depositional leaching or alteration. Recognizable grains are similar to those described above. possibly a reflection of considerable surface solution of carbonate.

Traces of dark black material associated with Upper Cretaceous sediments, originally identified as "asphaltite," was found to be low in organic carbon. Such zones are now interpreted as iron-rich, residual soil horizons,

It is interesting to note that in the shallow-water Upper Cretaceous limestones and dolomites no evidence of reef-building organisms was observed. On the basis of sedimentological parameters, carbonate petrography, and paleontological interpretations, the depositional environment appears to have been shallow shelf to supratidal for the upper few tens of meters of Upper Cretaceous platform carbonates penetrated at Sites 86, 94, and 95. Furthermore, the cyclical nature of partial sequences studied (Figure 9) suggests that essentially intertidal conditions prevailed to some extent. Pusey states that these miliolid-rich mudstones and wackestones are identical with restricted, shallow shelf deposits known from other portions of the Gulf of Mexico. The only major exception appears to be that echinoderm fragments are extremely rare at the drilled sites which implies even greater restriction and isolation from normal marine circulation. One is left to conclude that reef and associated facies lie either seaward of these sites or are poorly developed.

The presence of rudistid reef facies appears assured by rudistid debris seaward of the Campeche Scarp (Site 85). Site 3 of Leg 1 also encountered rudistid fragments in deep-water turbidites of Plio-Pleistocene age. It thus appears evident that reef facies either were, or are, present near the present margin of the Campeche Scarp. Following deposition of the shallow-water carbonates described above, the suggestion is that the carbonate platform was then emergent and quite possibly subjected to subaerial erosion. No transgressive phase of sedimentation accompanied by reef development could be discerned at the sites drilled, although such could have been removed by erosion. Subsequent deposition appears to have been comprised of relatively deep-water pelagic ooze, suggesting a drowning of the outer portions of the carbonate platform, essentially to present depths of water.

DEEP-WATER LIMESTONES

Deep-water limestones were recovered from Site 97 and consisted of (carbonate) pebbly mudstone apparently overlying interbedded calcilutite and calcisiltite, all of Early Cenomanian (Late Cretaceous) age. The pebbly mudstones consist of abundant clasts of limestone of various colors and hardness, generally recrystallized (micrite) chalk clasts, porous dolomite clasts of probable Early Cretaceous shelf origin, and mud clasts, often deformed, of slightly clayey to clayey calcilutite (sometimes similar to associated fine-grained interbeds of the sequence described). Paleontological study suggests that much of the detritus is shallow water in origin, containing retransported shallow-water forams. Several different ages of sediment are suggested on the basis of disaggregation of individual clasts. Present data suggest that (pelagic) slope sediments comprised an important, although not necessarily dominant, nearby source of clasts. The considerable amount of miliolid debris reported by McNeely (this volume) from these sediments would support a shelf-bank source.

The general occurrence of exotic clasts suspended in a matrix of mixed deep-water ooze-clay and "shallow-water" debris of variable size is common to deep-water sediments of many areas. The rather unique textural mix and fabric of pebbly mudstones have been generally ascribed to a gravity-dominated process known as low velocity mass flow, or simply as gravity mud slides of submarine origin. The association of these sediments with calcilutite containing a deep-water fauna is suggestive of nearby areas of high bathymetric relief, such as exist at present.

The underlying hard, dense, horizontally to vaguely laminated to sparsely mottled calcisiltites and calcilutites which occur in Cores 11 and 12 are more difficult to interpret. On the basis of Pusey's petrographic work, it appears that the dominant particle types contained within these sediments are fine-grained detrital carbonate and planktonic foraminifera tests, with rare, unbroken, thin-walled pelecypod shells, ostracod shells, and miliolids. Microscopically, laminae consist of fossil-rich micrite alternating with micrite. The micrite contains abundant particulate organic material up to 10 microns in size, consisting of translucent, brown globules. Lithologically, these limestones resemble similar lithologies from the mid-Paleozoic of the Ouachita fold belt of southeastern Oklahoma and west Texas, which are interpreted variously as moderate to deep water in origin.

The association of these rock types with carbonaceous organic-rich, radiolarian (?), microlaminated chert similar to various deep-water cherts of open ocean origin from Leg 1 (Beall and Fischer, 1969), and with interbedded, vaguely laminated, clayey, nannofossil-rich calcilutite of probable deep-water origin suggests that the dense limestones are lithified deep-water carbonate analogues of terrigenous clastic hemilaminites and laminites. The presence of deep-water limestones during a period when correlative shallow-water carbonates were undoubtedly accumulating on the nearby carbonate platforms is strongly suggestive that the area of Site 97 occupied a relatively deep-water position during Early Cretaceous time. This has important implications as to the structural evolution of the Gulf of Mexico in Cretaceous time and earlier.

PHYSICAL PROPERTIES OF SEDIMENTS

Any discussion of physical properties of sediments necessarily draws on other types of data such as mineralogy and textural composition. As used here, physical properties refer primarily to those measurements of physical parameters taken on board ship and include (1) bulk density as determined by GRAPE (Gamma-Ray Attenuation Porosity Evaluation), (2) natural gamma-ray emission, measured as counts per 75 seconds, (3) intermittent penetrometer tests which utilize measurement of depth of penetration of a weighted needle into sediment, (4) intermittent measurement of sonic velocity utilizing a "sediment velocimeter," (5) laboratory determination of water content, bulk density, and grain density of selected samples, and (6) laboratory determination of pore water salinity, as derived from measurement of selected, artificially consolidated samples. As will be reviewed in a subsequent section, chromatographic analysis of "natural gas" samples from selected cores was also carried out and might be termed a "physical property."

Continuous measurement of gamma-ray emission and density can be used to differentiate lithology on a detailed basis as well as demonstrating broad-scale variations in composition and degree of consolidation. Beall and Fischer (1969) have shown, in the case of Leg 1 sediments, examples of detailed differentiation of various lithologies. Enough of this type of data has now been obtained for the deep-water Gulf of Mexico to show statistically valid results.

Natural Gamma-Ray

Figure 10 compares average core barrel results of natural gamma-ray count versus per cent total carbonate, as taken from x-ray diffraction analysis. It should be pointed out that individual mineralogic samples are not necessarily representative for average composition of an entire

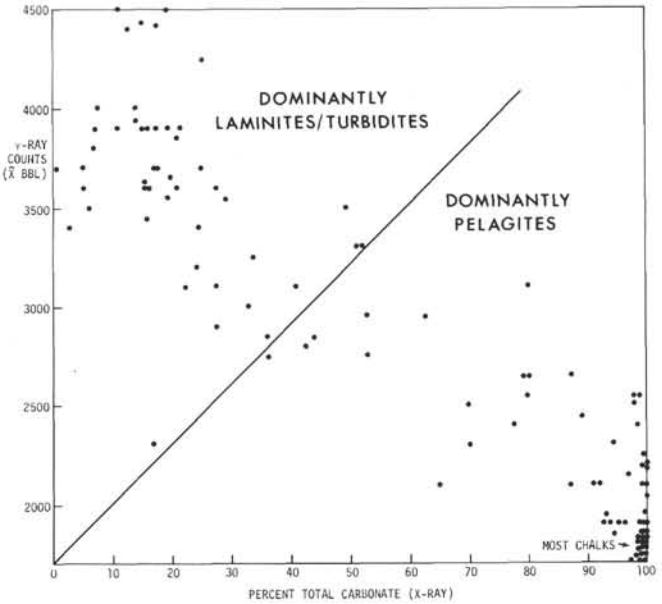

Figure 10. *Comparison of natural gamma-ray count versus percent total carbonate (from x-ray diffraction).*

core. Nevertheless, a pronounced inverse correlation between carbonate content and gamma-ray count can be noted. As shown on the figure, most of the samples of high gamma-ray count can be characterized as (terrigenous clastic-dominated) laminite or turbidite sequences, whereas the high carbonate sediments are characteristically pelagites. Also, note that most chalks result in plots with very low gamma-ray counts. Alternatively, a plot of gamma-ray count versus clay content would also show a marked correlation of similar degree. Zones of high gamma-ray emission and with high zeolite or volcanic glass content can also be cited as responsible for some of the variability shown.

Where core sampling is somewhat closely spaced, natural gamma-ray data can be used to characterize vertical sequences of rock, much in the same way that conventional gamma-ray surveys are used in subsurface geology. Figure 11 shows a cross section along the outer Yucatan platform (Sites 86, 94, and 95) where paleontological age data have been rather uniquely substantiated by gamma-ray correlation. In this case, it is readily recognized that correlative zones persist throughout the region. Post-Oligocene and pre-Upper Cretaceous units are generally more radioactive as compared to the remainder of the lower Tertiary. The missing upper Tertiary section at Site 95 is clearly shown by gamma-ray data. Increasing clay content toward Site 86 is thought to be responsible for increasing gamma-ray count in correlative beds, especially as seen in Pliocene and Paleocene intervals.

Other examples of gamma-ray correlation can also be cited. Tentative gamma-ray correlations were made between Site 91 and Site 87/3. In view of the different system used to date Site 3, a gamma-ray correlation would suggest that Cores 5 and 6 (330) from Site 3 are approximately equivalent, stratigraphically, to the base of Pleistocene sediments as described at Site 91 between Cores 8 and 9 (517). Further paleontological study of Site 3 will be necessary to confirm this correlation. As shown in Figure 7, such a correlation is important in resolving the stratigraphic position of the Campeche-Yucatan carbonate turbidite wedge, as seen at Site 87/3. This wedge of abyssal plain sediment does not appear to be present in terms of a carbonate-dominated lithology at Site 91.

Penetrometer

A penetrometer measurement basically defines the ability of a sharp, weighted needle to penetrate sediment. Such measurements, calibrated in thousandths of a millimeter, appear to adequately define the state of consolidation of sediments, although they are difficult to relate to conventional engineering measurements in quantitative terms. For purposes of comparison, penetrometer measurements correspond well with geological observations as to state of consolidation and are reproducible within a small experimental error. An empirical scale of consolidation has been assigned to penetrometer data for the Gulf of Mexico (Beall and Fischer, 1969). Readings between 0 and 10 ($\times 10^{-3}$ mm) are designated as *stone,* 10 to 30 are *semi-consolidated,* and sediments with penetration greater than 30 are *unconsolidated.*

Figure 12 shows a summary plot of penetrometer results for Leg 10 (including data from Leg 1). For purposes of comparison, data have been grouped into those categories previously used for comparing mineralogic data. Those categories are (1) slope (pelagic) sediments, (2) abyssal plain or rise sediments, (3) sediments accumulated on salt structures, and (4) the Straits of Florida site. Note that the abyssal plain and rise muds are the least consolidated as compared to the less penetrable carbonate sediments. Penetrometer tests in the pelagic carbonate sediments show the appearance of "chalk" at about 400 meters (an average depth for the sites studied).

It is interesting to note that the "salt dome sediments," which reflect an essentially pelagic mode of deposition for the most part, are more consolidated than the "normal" pelagic sediments. These sediments appear to be "over-consolidated" with respect to "normally consolidated" sediments of similar lithological composition. This subject will be continued under the discussion of bulk density data.

The Straits of Florida site is somewhat unique, both in sedimentological setting-sediment type and in terms of penetrometer results. Here the presence of "soft" chalk was first noted at a depth of 200 meters below the sediment-water interface, demonstrating a strong dependence of a "chalk" lithology on composition. Sediment above this level is also somewhat "over-consolidated," suggesting the possibility that either slow rates of deposition and-/or concurrent intermittent erosion are somehow responsible. Deep-water limestones and associated pebbly mudstones at the base of Site 97 are generally quite consolidated, with the exception of thin interbeds of pelagic ooze, which may represent disturbance during coring.

Bulk Density

Bulk density data are categorized in the same way as the penetrometer data (Figure 13). Abyssal plain sediments, all of post-Miocene age and largely comprised of

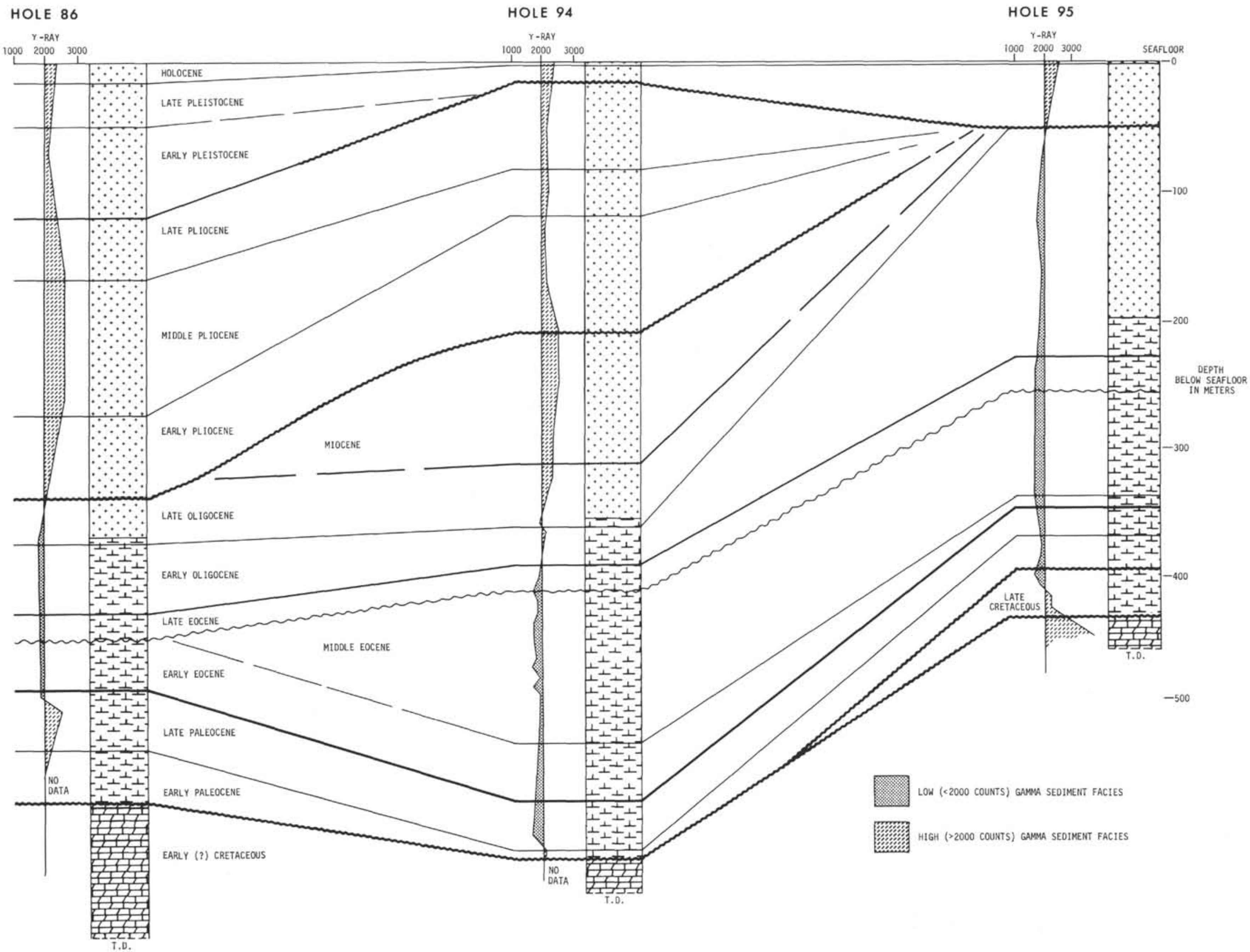

Figure 11. *Comparison of paleontological and gamma-ray correlation along the outer Yucatan platform.*

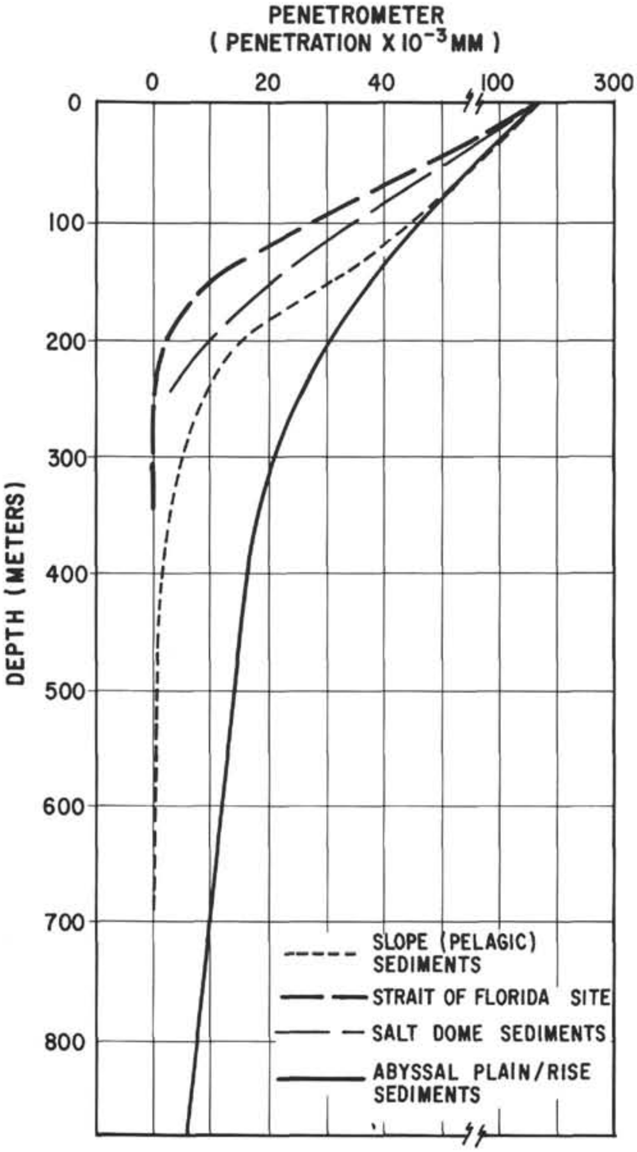

Figure 12. *Summary plot of penetrometer results versus sedimentological assemblages used in this paper; Legs 1 and 10 combined for deepwater Gulf of Mexico sediments.*

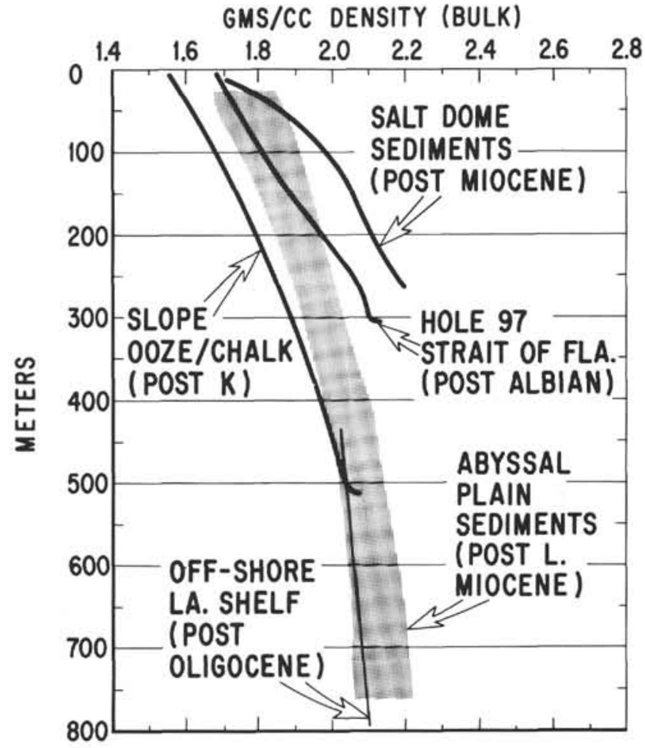

Figure 13. *Summary plot of bulk density versus sedimentological assemblages used in this paper; Legs 1 and 10 combined for deepwater Gulf of Mexico sediments.*

terrigenous clastic mud/clay, define a somewhat broad band of bulk densities with increasing depth. Much of the variation noted is apparently due to lithologic variability, e.g. carbonate-bearing units versus terrigenous clay-bearing units versus quartzose silt/sand-bearing units, but nevertheless a definite data field is apparent. Site 1 essentially defines the upper limit of bulk density in the field whereas Site 89 defines the lower boundary.

Abyssal plain and rise sediments can be compared with sediments recovered from the crest of salt structures, where considerably denser sediments are apparent. One such example is from Site 2 (Leg 1), where a thin section of Plio-Pleistocene clay and clayey ooze directly overlies caprock. Lithological composition appears to be of only secondary importance in such cases, however, for sediments from Site 92, with a similar bulk density trend, is comprised almost totally of terrigenous clastic sediments. These data, in conjunction with data from at Site 88, suggest again that sediment from the crests of salt structures exhibit "over-consolidation" with respect to other sediment categories and present depth of burial.

The slope ooze and chalk are characterized by somewhat low bulk densities even in the consolidated chalk intervals. The high porosities noted in this type of sediment are apparently related to the high percentage of biogenic debris present, notably foraminiferal tests and nannofossil debris. At depth, the older chalks and oozes terminate abruptly at approximately the Early-Late Cretaceous boundary. Sediments below this point are hard, recrystallized, moderately dense limestones and dolomites. Bulk densities were not determined on this material but are known to be high from observation and relatively low porosity values as determined from thin section data.

Site 97, from the Straits of Florida, again represents somewhat of an anomaly with respect to other sites studied. The sequence of relatively low density pelagic oozes and chalks superimposed on rather dense pebbly mudstones and limestones with interbedded minor chert is apparent. The dense carbonate rock fragments present in the pebbly mudstones are apparently responsible, at least in part, for the high bulk density readings reached in this lower interval.

Consolidation and Pore-water Composition

Interpretations as to consolidation of clastic muds and clays from the abyssal plain can be made by combining bulk density and penetrometer data. Note that the change from rapid consolidation with depth (or low bulk densities and high penetrometer values) to lesser rates of consolidation with depth (or high bulk densities and low penetrometer values) takes place at approximately 400 meters (about 1250 feet) (see site summaries, Sites 90 and 91). These changes take place in what has previously been described as "Stage I" consolidation or simple expulsion of pore water. As such, these sediments have not been buried to great enough depths to experience the onset of NaCl filtration. Such is subtantiated by shipboard salinity determination of rapidly squeezed pore fluids. Manheim (1969) has shown, on the basis of most Deep Sea Drilling Project sediment fluid extractions to date, that NaCl filtration does not appear to be operative at the shallow depths cored.

Examination of sediments from the crests of salt structures (Sites 2, 92, and 88) suggests that salt diffusion from underlying salt can be common in deep-water sediments. These sediments, as previously discussed, generally appear to show anomalously high bulk densities at shallow burial depths along with an "over-consolidated" appearance as documented by penetrometer measurements.

Site 92 had been previously suggested to be underlain by salt, as based on seismic profiling (Beall, 1968). Figure 14 shows a detailed summary of Site 92, including generalized lithology as well as bulk density, penetrometer values, and pore water salinity as determined by the shipboard chemist. Note that the sequence can be separated into an upper unit of unconsolidated to semi-consolidated Upper Pleistocene clay and mud which overlies a lower section of semi-consolidated to consolidated clay mud and mudstone claystone of Early Pleistocene age. The top of the salt (or caprock) was calculated to be at a depth of approximately 300 meters, based on seismic profiling.

Physical measurements at Site 92 show a relatively consistent and rapid increase in consolidation with depth. There is a somewhat more rapid increase in bulk density at about 200 meters, which suggests that there may be some missing section. Sediment below that level also shows annealed vertical fractures, especially toward the base of the hole. Salinity determinations were carried out on cored sediment using the techniques of Manheim et al. (1969). Results clearly show a consistent increase of salinity with depth, reaching a level of about five times normal seawater at a depth of approximately 200 meters below the sediment-water interface. This rapid and pronounced increase in salinity is apparently due to diffusion of salt through the capping sediments. The mudstones which overlie salt are of deep-water origin and very young in age, thus removing from consideration effects which should be ascribed to age, subaerial exposure, or invasion via permeable sandstones of older age, as is often the case in shelf and onshore settings. The results cited above are quite comparable to those reported by Manheim and Bischoff (1969) for sediments on the upper continental slope of offshore Texas.

These results clearly illustrate the ability of consolidating clays and muds to transmit hypersaline solutions. Furthermore, it would appear that this process of diffusion somehow facilitates "over-consolidation" of sediments. It

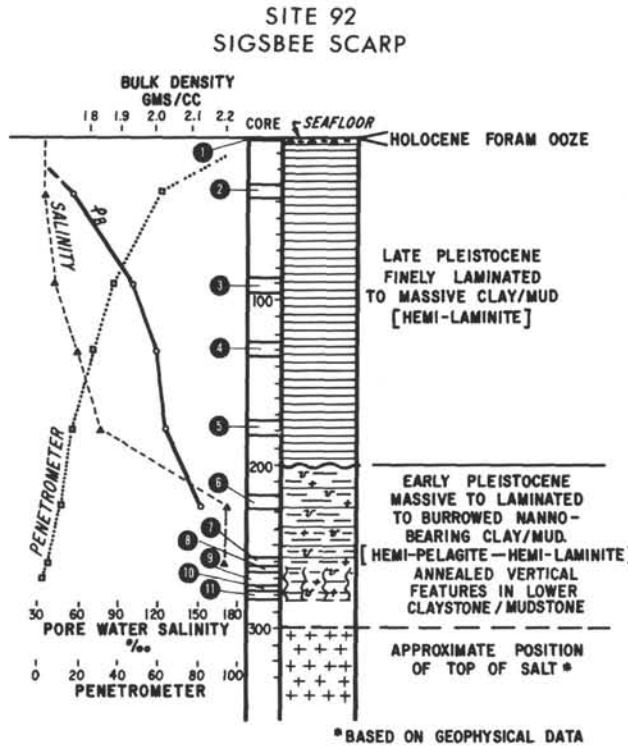

Figure 14. *Lithology and physical and chemical properties, Site 92.*

may be that because of saturation of grain boundary bonding sites, mechanical rotation of particles is facilitated. Diagenetic cementation as related to possibly higher thermal gradients on salt structures might also be cited. The data cited above, in conjunction with these speculations, are yet another example of how data on deep-water sediments may help to provide answers to puzzling geological phenomena in shallow-water sequences where a considerably greater range of variables is involved.

Natural Gas

Odors of natural gas were detected in a number of cores early in Leg 10, suggesting that continuous monitoring of free gas from within the core liner would be of significance. Site 88, as well as later sites, showed measurable quantities of methane, and minor amounts of ethane and hydrogen sulfide. Volumes of methane and ethane appear to reach a maximum at levels of approximately 100 meters, declining downwards. Hydrogen sulfide gas appears to be most abundant in very shallow cores.

The presence of natural gas is intriguing, in that at least two origins can be hypothesized. The first hypothesis might be that these hydrocarbons (methane and ethane) represent simple diffusion from the underlying caprock through the low permeability ooze or clay up to the sediment surface. In such a case, however, one might expect a continuous increase in the amount of hydrocarbon gas detected as well as a continuous increase in the proportion of heavier hydrocarbons. Such does not appear to be the case. The second hypothesis, and the one favored here, is that the natural gases represent the generation of in situ natural gas through organogenic processes, probably bacterial. Evidence of reducing conditions is taken from the greenish gray to gray pigmentation of the sediment as well as the presence of fecal and FeS material throughout. The decline of ethane as well as the decline of total gas with depth suggests that generation may also be inhibited at greater depths of burial (with lesser permeability and porosity). The total volume of natural gas in these sediments must be small in comparison with the volume of sediment and fluid while the relatively low permeability of enclosing sediment suggests that any vertical diffusion of hydrocarbons is a slow process. We have thus concluded that the gas in this case, is biogenic in origin.

REFERENCES

Beall, A.O. and Fischer, A.G., 1969. Sedimentology. *In* Ewing, W.M., Worzel, J.L. et al., 1969. Initial Reports of the Deep Sea Drilling Project, Volume I. Washington (U.S. Government Printing Office). 521.

Beall, Arthur O., Jr., 1968. Deep sea drilling project throws new light on Gulf sedimentation. Oil and Gas Jour., Dec. 1, 1969. 94.

Beall, A.O., Jr., 1970. Textural differentiation within the fine sand grade. J. Geol. **78**, 77.

Behrens, E.W., 1965. Environment reconstruction for a part of the Glen Rose Limestone, central Texas. Sedimentology. **4**, 65.

Griffith, L.S., Pitcher, M.G. and Rice, G.W., 1969. Quantitative environmental analysis of a Lower Cretaceous reef complex. Soc. Econ. Paleontologists and Mineralogists, Spec. Pub. 14. 120.

Manheim, F.T. and Bischoff, J.L., 1969. Geochemistry of pore waters from Shell Oil Co. drill holes on the continental slope of the Gulf of Mexico. *In* Geochemistry of subsurface brines (Symposium). E.E. Angino and G.K. Billings (Eds.). Chem. Geol.

Manheim, F.T., Sayles, F.L. and Friedman, I., 1969. Interstitial water studies on small core samples, Deep Sea Drilling Project, Leg I. *In* Ewing, W.M., Worzel, J.L. et al., 1969. Initial Reports of the Deep Sea Drilling Project, Volume I. Washington (U.S. Government Printing Office). 403.

PLATE 1

Figure 1	Sample 85-1-6 (3 cm); plain light. Late Pleistocene, zeolite crystals, one twinned (in center), in a quartzose marl silt.
Figure 2	Sample 85-5-2 (80 cm); plain light. Late Pleistocene, calcareous clayey medium sand. Included in slide are an abraded calcite prism from a pelecypod shell (in center of plate), orthoclase feldspar (0), plagiocalse feldspar (P), chert grain (C), micritic intraclasts (large, rounded to subrounded, opaque grains), and quartz (most of the remaining grains). The smaller of the two plagioclase grains is badly altered. Following figure from same slide.
Figure 3	Sample 85-5-2 (80 cm); plain light. Late Pleistocene, detrital calcite(C), plagioclase with rutile inclusions (P), microcline(M), green hornblende(H), and a silicic volcanic rock fragment in a calcareous turbidite sand.
Figure 4	Sample 85A-2(CC); plain light. Late Pleistocene, dolomite rhombs in terrigenous clay rich in macerated plant detritus.
Figures 5, 6	Sample 86-2-1 (65 cm); crossed-polarized (Figure 5) and plain (Figure 6) light. Early Pleistocene, angular glass shard (center), faecal pellet (P), single foraminifer chamber (F), calcitic molluscan fragment (M), and larger coccoliths (C), in nannoplankton chalk ooze. Clay-size detrital carbonate is abundant (Figure 6).
Figure 7	Sample 86-3-2 (10 cm); plain light. Middle to Late Pliocene, foram-bearing nannoplankton chalk ooze. Foraminifera, except for one on right, are mostly fragmented. Six-rayed discoasters are common. Larger coccoliths are oval-shaped. Zeolite crystal in upper right (Z).
Figure 8	Sample 86-5-2 (71 cm); plain light. Late Oligocene, volcanic glass(g) present in coccolith chalk ooze. Triaxon sponge spicule and silt-size radiolarian fragments can be seen.
Figures 9, 10	Sample 86-7-5 (2 cm); plain (Figure 9) and crossed-polarized (Figure 10) light. Late Paleocene, calcitic pentaliths of the coccolith *Braarudosphaera* (P) and fragments thereof are abundant consituents along with other coccoliths. Also present are euhedral crystals of zeolites (Z) and dolomite (D). The sediment is a nannoplankton chalk ooze.
Figure 11	Sample 87-1-1 (136 cm); plain light. Late Miocene, large, sub-angular, brown biotite grain in a marl sandy silt. A few silt-size zeolites (Z) are visible.
Figure 12	Sample 87-1-2 (14 cm); plain light. Large, fresh, green hornblende grain in a marl sandy silt (Late Miocene).

PLATE 1

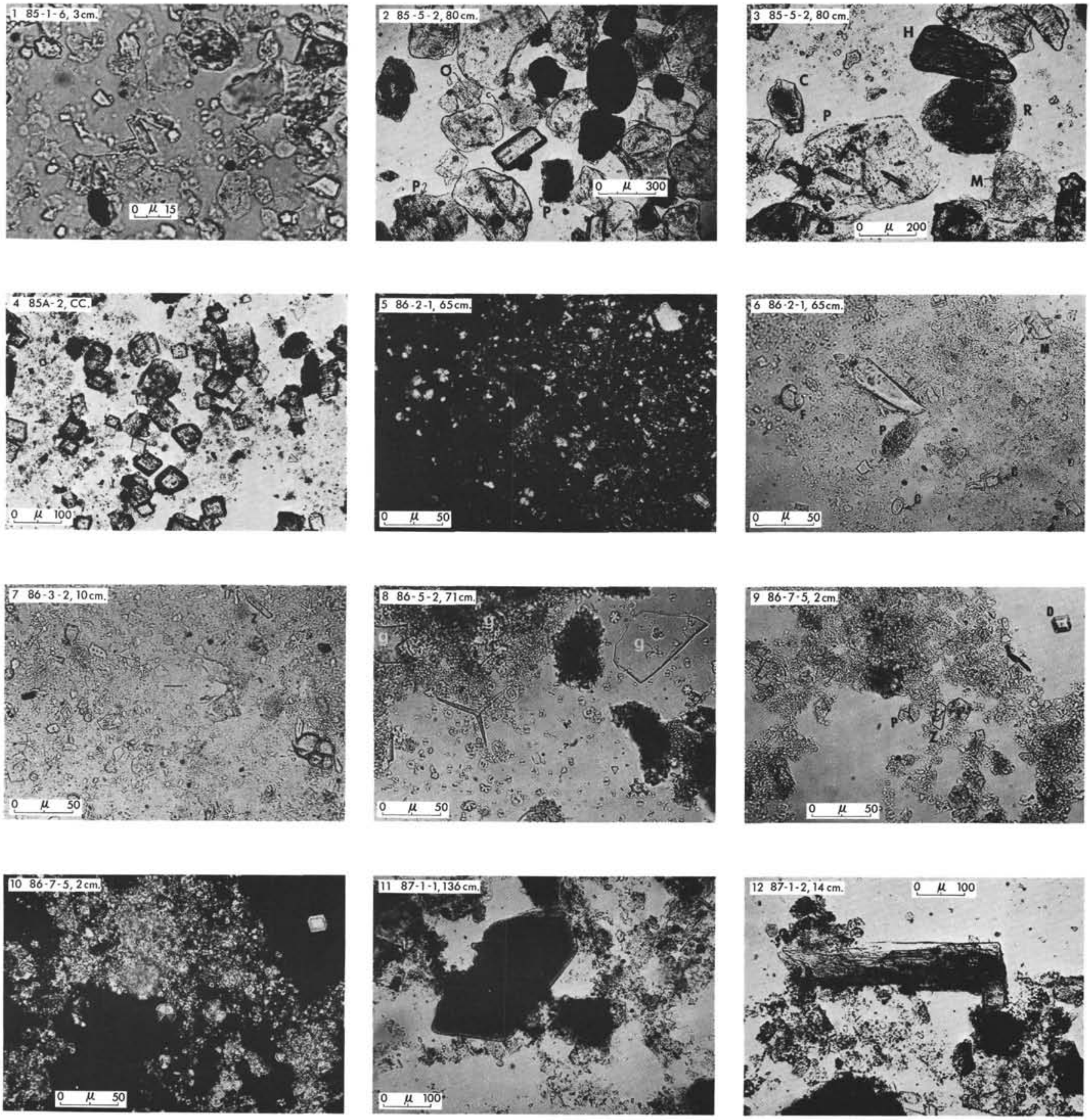
1 85-1-6, 3cm.
0 μ 15
2 85-5-2, 80cm.
0 μ 300
3 85-5-2, 80 cm.
0 μ 200
4 85A-2, CC.
0 μ 100
5 86-2-1, 65cm.
0 μ 50
6 86-2-1, 65cm.
0 μ 50
7 86-3-2, 10cm.
0 μ 50
8 86-5-2, 71cm.
0 μ 50
9 86-7-5, 2cm.
0 μ 50
10 86-7-5, 2cm.
0 μ 50
11 87-1-1, 136cm.
0 μ 100
12 87-1-2, 14 cm.
0 μ 100

PLATE 2

Figure 1	Sample 88-1-1 (135 cm); crossed-polarized light. Late Pleistocene, nannoplankton chalk ooze with large Carlsbad-twinned K-feldspar grain and smaller chert grain (C). Detrital (probably biogenic) carbonate grains, highly birefringent, equant to spindle-shaped, are common in the 10-15 micron size range.
Figure 2	Sample 88-2-5 (80 cm); plain light plus reflected light. Late Pleistocene, spherulitic pyrite filling two chambers of globigerinid foraminiferal test. Sediment is a nannoplankton chalk ooze with fragments of foraminifera and, less frequently, pteropods (p).
Figure 3	Sample 89-1-2 (97 cm); plain light. Late Pleistocene, pumice (very vesicular) (center and upper right) and abundant other angular, glassy ash particles in ashy nannoplankton chalk ooze.
Figures 4, 5	Sample 89-4-4 (75 cm); plain (Figure 4) and crossed-polarized (Figure 5) light. Middle Pliocene, untwinned sanidine (S) and volcanic glass shard (G) in nannoplankton chalk ooze. Discoasters and coccoliths present; the latter dominate.
Figure 6	Sample 89-4-6 (111 cm); plain light. Middle Pliocene, clear, brown, and very iron-rich (essentially opaque) volcanic glass shards. Angularity is high, sorting very poor; median diameter probably in fine-sand range.
Figure 7	Sample 90-1-4 (102 cm); plain light. Late Pleistocene, angular and frequently grooved glass shards in ash-bearing nannoplankton chalk clay. Fragmented or entire foraminifera (f) also present. Aggregates of very fine carbonate (p) are probably faecal pellets.
Figure 8	Sample 90-5-4 (100 cm); plain light. Late Miocene, terrigenous clay with common euhedral, silt-size pyrite; bladed, clear zeolite crystals (commonly twinned); and occasional green glauconite pellets (G).
Figure 9	Sample 90-10-1 (50 cm); plain light. Late Middle Miocene, quartzose marl sandy silt, poorly sorted and with an unstable grain assemblage including green hornblende (h), plagioclase (P), garnet (G), rutile (R), zircon (Z), micritic clasts (m), macerated plant matter (C), in addition to quartz, other feldspar, detrital carbonate, rock fragments, and others.
Figure 10	Sample 90-12 (CC); plain light. Middle Miocene, brown biotite (b), quartz (Q), and abundant zeolites (commonly euhedral, 6-sided, subequant to bladed) in zeolitic, calcareous, sandy mud. Following figure from same slide.
Figure 11	Sample 90-12 (CC); crossed-polarized light. Middle Miocene, fresh, normally zoned plagioclase crystal, found in a zeolite-bearing, calcareous sandy mud.
Figure 12	Sample 91-20-2 (80 cm); plain light. Middle Miocene, rounded sand grain in center is of volcanic glass (isotropic, negative relief); conchoidal chip in upper part of grain was proabably incurred during turbidity flow transit. Orthoclase (O) and an unidentified volcanic rock fragment (V) are also present in the field.

PLATE 2

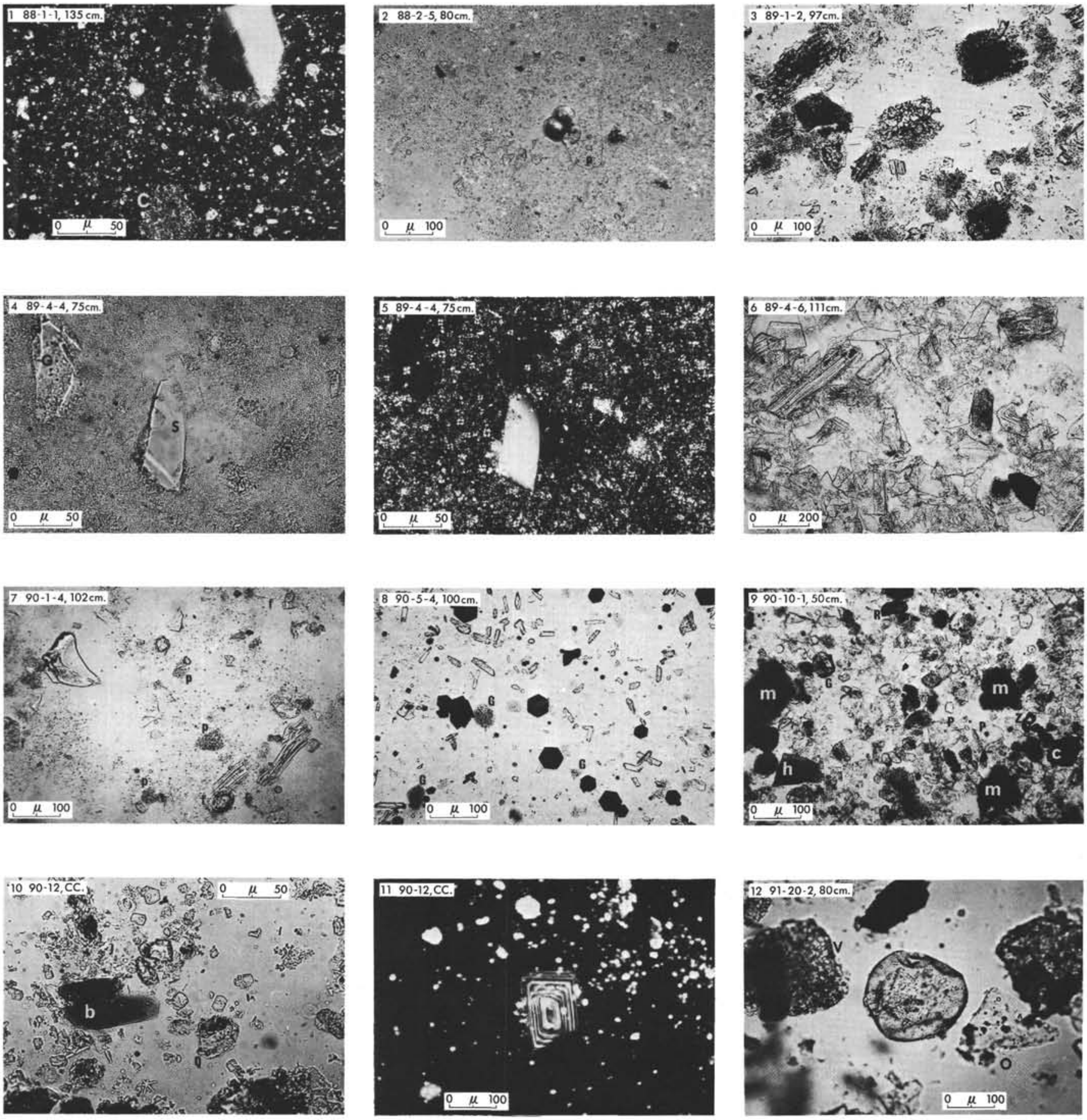
1 88-1-1, 135 cm.
C
0 μ 50
2 88-2-5, 80cm.
0 μ 100
3 89-1-2, 97cm.
0 μ 100
4 89-4-4, 75cm.
G
S
0 μ 50
5 89-4-4, 75cm.
0 μ 50
6 89-4-6, 111cm.
0 μ 200
7 90-1-4, 102cm.
P
P
P
0 μ 100
8 90-5-4, 100cm.
G
G
G
G
0 μ 100
9 90-10-1, 50cm.
R
m
G
m
P
P
Z
c
h
m
0 μ 100
10 90-12, CC.
0 μ 50
b
11 90-12, CC.
0 μ 100
12 91-20-2, 80cm.
V
O
0 μ 100

PLATE 3

Thin Sections

Figure 1 Sample 90-13-4 (35 cm); plain light. Middle Miocene, large, fresh, basaltic rock fragment with plagioclase laths, from turbidite sand.

Figure 2 Sample 90-13-4 (35 cm); crossed-polarized light. Middle Miocene, rock fragment of weakly metamorphosed (chlorite grade), sandy quartzose siltstone. From poorly sorted, unstable, turbidite sand.

Figure 3 Sample 90-13-4 (35 cm); crossed-polarized light. Middle Miocene, exceedingly fresh, fairly calcic plagioclase grain from the turbidite sand.

Figure 4 Sample 90-13-4 (35 cm); plain light. Middle Miocene, large, subrounded pelecypod fragment showing preservation of crossed-lamellar microstructure (probably aragonitic) and extensive marginal boring (B) by endolithic blue green algae. Borings have been subsequently infilled with micritic carbonate, producing a micritic envelope around the grain. Numerous borings are seen to penetrate more deeply into the fragment. Algal borings indicate derivation of the mollusc fragment from shallow water, within the photic zone.

Figures 5, 6 Sample 90-13-4 (35 cm); plain (Figure 5) and crossed-polarized (Figure 6) light. Middle Miocene, large spherulitic volcanic rock fragment in texturally very immature and compositionally very unstable turbidite sand. Rock fragment, acidic to intermediate in composition, is relatively fresh.

PLATE 3

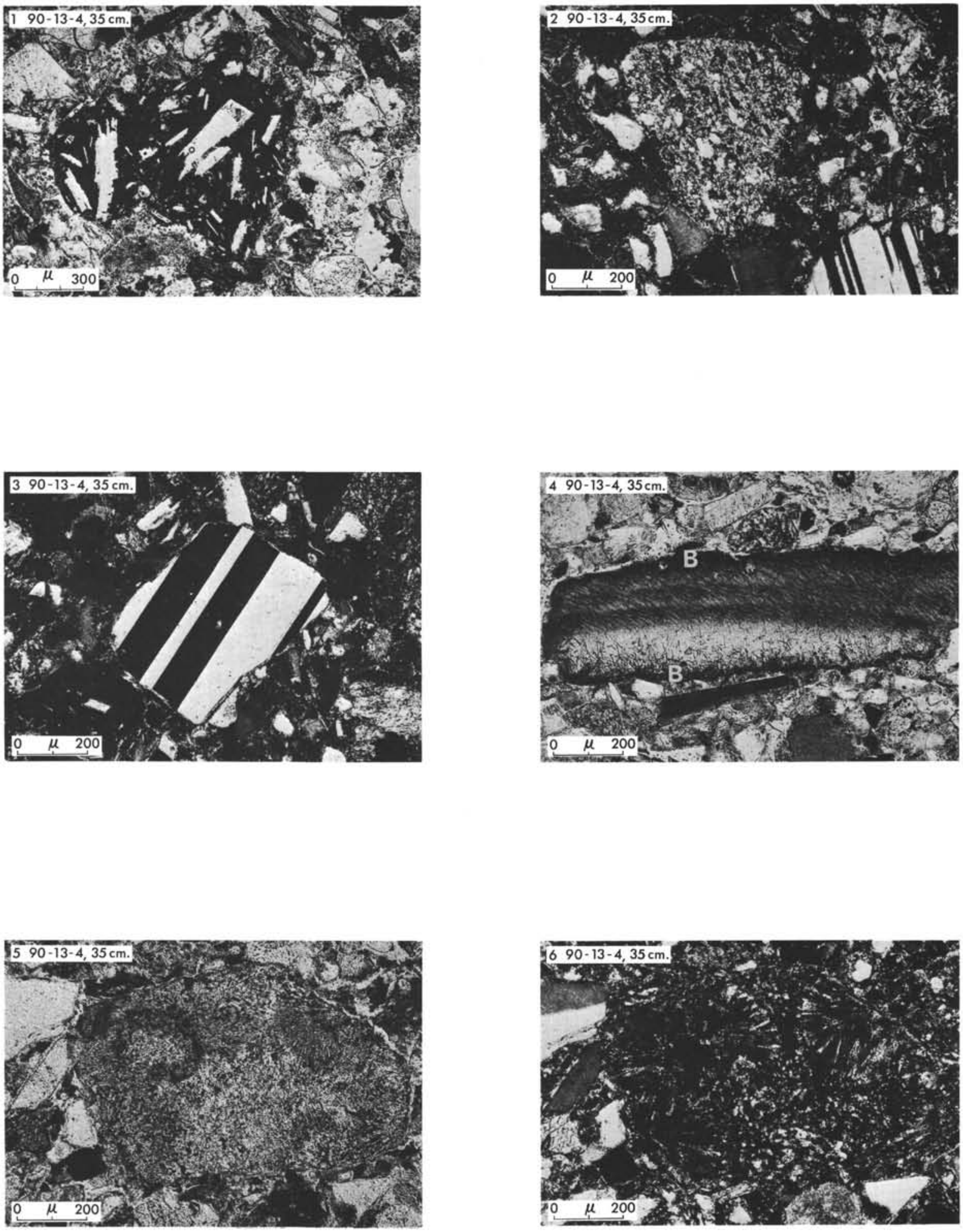
1 90-13-4, 35 cm.
0 μ 300
2 90-13-4, 35 cm.
0 μ 200
3 90-13-4, 35 cm.
0 μ 200
4 90-13-4, 35 cm.
B
B
0 μ 200
5 90-13-4, 35 cm.
0 μ 200
6 90-13-4, 35 cm.
0 μ 200

PLATE 4

Figures 1, 2	Sample 92-9 (CC); plain (Figure 1) and crossed-polarized (Figure 2) light. Single-crystals, spherulitic, of carbonate, probably siderite. These crystals are also present in the terrigenous clay of sample 92-7-1 (123 cm). Early Pleistocene.
Figure 3	Sample 94-1-2 (80 cm); plain light. Late Pleistocene, aragonitic didemnid tunicate spicules (T), calcitic molluscan prism (M), foraminifera, glass shard (G), faecal (?) pellets (P), and a siliceous sponge spicule (S) in a foram-bearing nannoplankton chalk ooze.
Figure 4	Sample 94-11-6 (5 cm); plain light. Late Oligocene, opaline sponge spicules (S), diatom frustule (D), volcanic glass (G), and foraminifera (F) in calcareous nannonplankton organic ooze.
Figure 5	Sample 94-35-1 (147 cm); crossed-polarized light. Late Paleocene, subhedral, zoned sanidine crystal in montmorillonitic clay. The sanidine is apparently the remnant of a volcanic ash, the glass of which has altered to montmorillonite.
Figure 6	Sample 94-38 (CC); crossed-polarized light. Cretaceous, Late Albian (?), detrital, silt-size carbonate (calcite) of unknown derivation. Possibly produced by breakdown (through bioturbation?) of pentalith coccoliths? Relatively well sorted chalk mud. Could also be the product of shallow-water calcareous algol productivity. Considered a shallow-water sediment.
Figure 7	Sample 95-5-4 (42 cm); plain light. Early Oligocene, predominantly foram-nannoplankton chalk ooze. Foraminifera commonly obscured by coating of very fine coccoliths or discoasters. Siliceous sponge spicules (one antler-shaped), and large glass shard (G) also visible.
Figure 8	Sample 95-8-6 (100 cm); plain light. Middle Eocene, spicule-bearing foram nannoplankton radiolarian marl ooze. Radiolaria, commonly coated with nannoplankton and fragmented clay and fine-silt-size skeletal debris, are dominant in this picture. Foraminifera and straight sponge spicules also visible.
Figure 9	Sample 95-12-1 (106 cm); plain light. Early Paleocene, small bladed zeolite crystals and larger, subequant volcanic glass in zeolite-bearing, ashy, calcareous sandy mud. The glass has a general corroded appearance and appears to be altering to clay.
Figure 10	Sample 95-13-3 (85 cm); crossed-polarized light. Cretaceous, late Campanian, spindle-shaped calcite grains of unknown derivation in chalk mud. Grains average 2-4 microns by 10-40 microns. Fair sorting.
Figure 11	Sample 96-3-5 (85 cm); plain light. Early Eocene, ash-bearing organic marl ooze, with a mixture of radiolaria (R), silicoflagellates (S), volcanic shards (G), foraminifera (F), and calcareous coccoliths (C).
Figure 12	Sample 96-5-1 (20 cm); plain light. Late Paleocene, radiolarian fragments (R) and even some of the zeolite crystals (Z) in this slide appear to be corroded. Primarily a coccolith chalk ooze.

PLATE 4

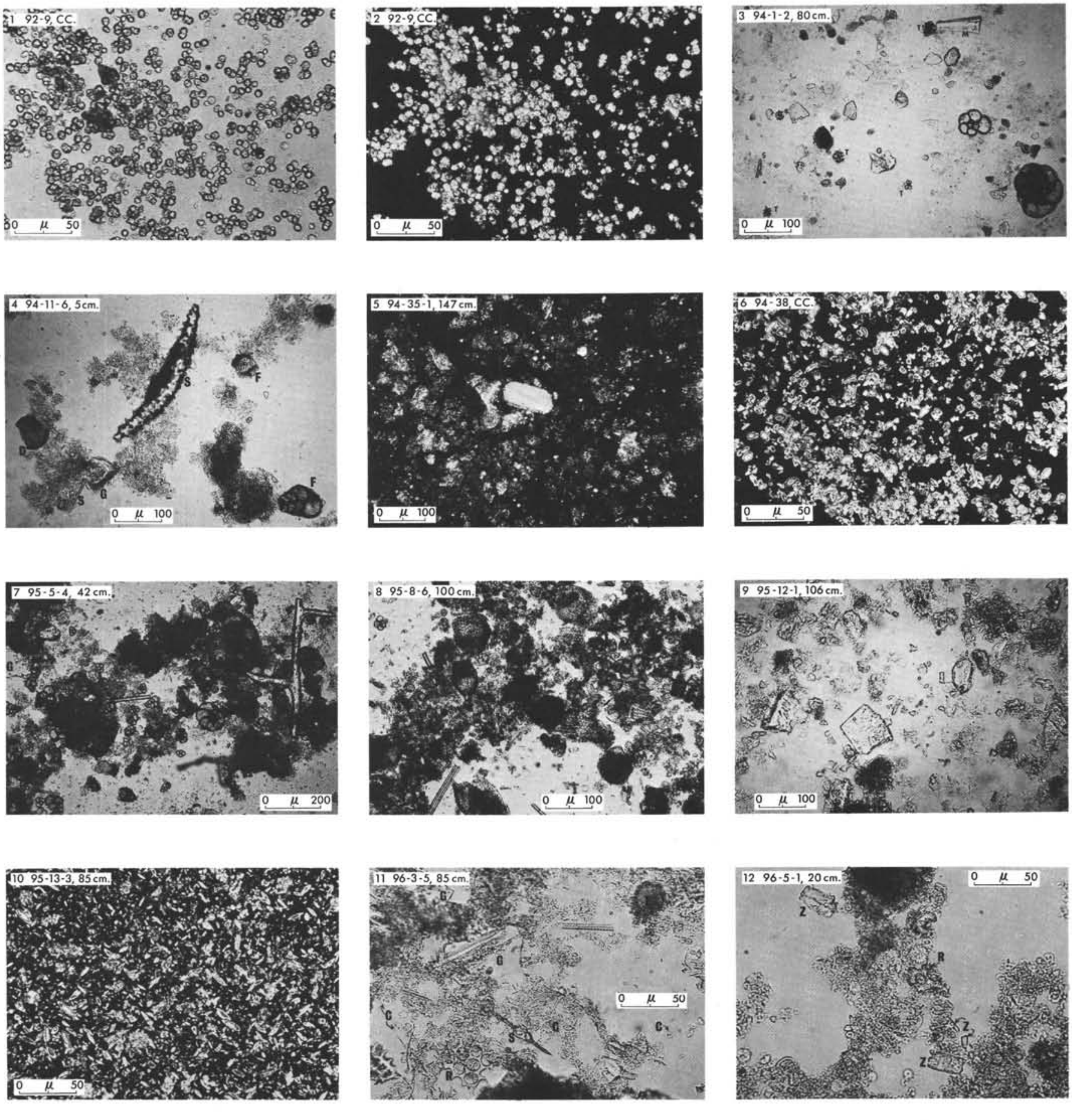
1 92-9, CC.
0 μ 50
2 92-9, CC.
0 μ 50
3 94-1-2, 80 cm.
0 μ 100
4 94-11-6, 5 cm.
0 μ 100
5 94-35-1, 147 cm.
0 μ 100
6 94-38, CC.
0 μ 50
7 95-5-4, 42 cm.
0 μ 200
8 95-8-6, 100 cm.
0 μ 100
9 95-12-1, 106 cm.
0 μ 100
10 95-13-3, 85 cm.
0 μ 50
11 96-3-5, 85 cm.
0 μ 50
12 96-5-1, 20 cm.
0 μ 50

PLATE 5

Thin Sections

Figure 1	Sample 96-4-1; plain light. Late Paleocene, chert replacement of carbonate ooze. Globigerinid foraminifer in matrix of opal-alpha cristobalite (o-a). Foram wall structure fairly well preserved even though replaced by chalcedony. Chalcedony (c) also fills light-colored areas of chambers. Foram chambers are coated with a very fine mosaic of alpha cristobalite (a), has large negative relief relative to chalcedony and has replaced opal. Light blotches outside the foram are recrystallized radiolaria and/or sponge spicules.
Figures 2, 3	Sample 97-6-1 (40 cm); plain (Figure 2) and crossed-polarized (Figure 3) light. Late Cretaceous, Cenomanian, patchy, irregular silica front in foram-nannoplankton chalk. Silicified portion of rock is in upper half. Opal-cristobalite-rich matrix in silicified zone is still largely isotropic; hence its dark appearance in the cross-polarized photograph (B). Porosity in unsilicified zone is largely in form of unfilled foram chambers. Opal-cristobalite and sometimes chalcedony have filled these pores and destroyed porosity in silicified area. Patchy replacement probably due to bioturbation of original chalk ooze.
Figure 4	Sample 97-12-1, 337 m (?) crossed-polarized light. Late Cretaceous, Cenomanian, light colored chert in lower half of picture changes upward, abruptly into a dark, carbonaceous zone which marks the leading edge of the silica front. The contact between the silica front and the unaltered chalk is relatively sharp and parallel to internal sediment stratification. Radiolaria, foraminifera, and sponge spicules, shown as ghosts in the black organic-rich zone, have been completely replaced or recrystallized to alpha quartz. Many of the siliceous microorganisms in the chalk have been replaced by calcite.
Figures 5, 6	Sample 97-12-1, 333 m (?); crossed-polarized light. Late Cretaceous, Cenomanian, intensive silicification of thinly laminated chalk. Except for discontinuous organic-rich (carbonaceous) laminae and occasional ghosts of foraminifera and radiolaria, the chert is a mosaic of microcrystalline alpha quartz. Foraminifera, especially the larger ones (B), are commonly infilled with fibrous chalcedony (forming a thick layer near the outer chamber wall) and mosaic, subsequent alpha quartz (in the center of the foram). Internal wall structure of the foram has been destroyed.

PLATE 5

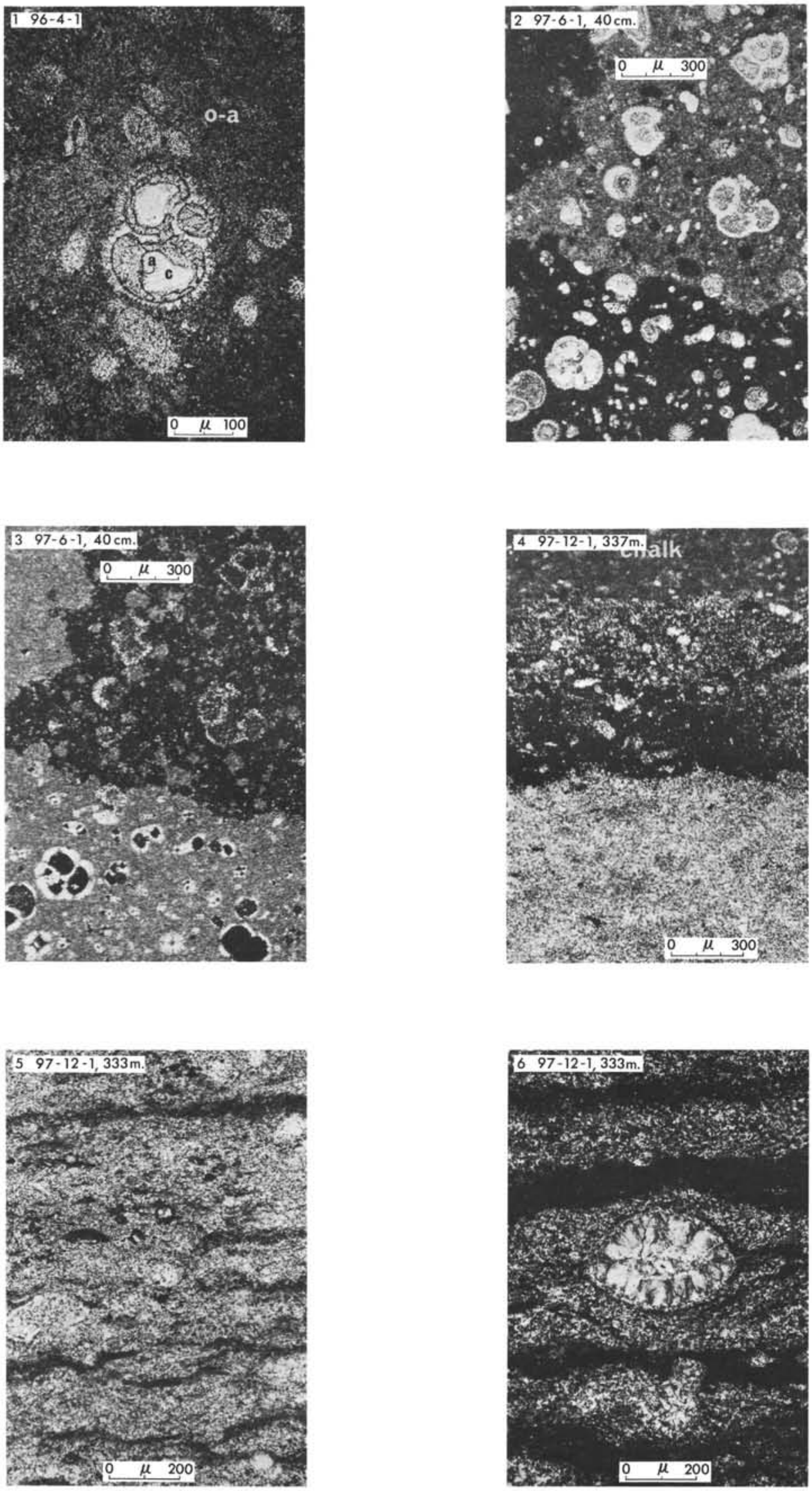
1 96-4-1
o-a
a
c
0 μ 100
2 97-6-1, 40 cm.
0 μ 300
3 97-6-1, 40 cm.
0 μ 300
4 97-12-1, 337m.
chalk
0 μ 300
5 97-12-1, 333m.
0 μ 200
6 97-12-1, 333m.
0 μ 200

PLATE 6

Plain light.

Figure 1	10-94-39 (31-47 cm); *pelletoidal packstone* (shallow marine shelf). Grains are pelletoids (a) lithoclasts (b), miliolids (c), ostracods and mollusks. Microspar mud matrix is half altered to dolomite in 10 to 50 micron rhombs. Mollusks are selectively leached, bulk composition of whole rock (by X-ray) is 71 per cent calcite and 29 per cent dolomite.
Figure 2	10-94-39 (65-71 cm); Plain light. *Miliolid wackestone* (low energy, semi-restricted marine shelf). Grains are miliolids (a), ostracods (b), orbitolinid forams (c), and pelecypods. Matrix is micrite. Bulk composition is 100 per cent calcite.
Figure 3	10-94-39 (74-83 cm); plain light. *Orbitolinid packstone* (very shallow, restricted marine shelf). Grains are large dicyclinid and orbitolinid forams (a), miliolids, pelecypods, red algae, ostracods, and other small forams (b). Matrix consists of micrite with numerous grain-sheltered voids (now spar-filled).
Figure 4	10-94-39 (74-83 cm); plain light. *Red algal nodule.* High magnification of coralline alga showing cellular structure.
Figure 5	10-94-39 (112-117 cm); plain light. *Stromatolitic mudstone* (supratidal mudflat). Laminae of miliolid-rich wackestone alternating with dark micrite laminae. Near-vertical desiccation cracks concentrated in specific layers and terminated abruptly by continuous micrite layers. The miliolids have been preferentially leached relative to hyaline forams, mollusks, and ostracods. Bulk composition is 95 per cent dolomite and 5 per cent calcite (the mollusks are calcite).
Figure 6	10-94-39 (139-146 cm); plain light. *Miliolid grainstone* (shallow marine, moderate energy). Consists of large miliolids of many types, especially *Nummoloculina* (a), other small forams (b), and pelecypods. Spar matrix. Bulk composition is 100 per cent calcite.
Figure 7	10-94-40 (CC); crossed-polarized light. *Miliolid grainstone* (shallow marine, moderate energy). Note dolomite rhombs as partial cement. Porosity is very high (approximately 25%).
Figure 8	10-95-21 (134-142 cm); crossed-polarized light. *Dolomite* (? low energy). Variable rhomb sizes and iron staining suggest that the original rock was a mottled mud or wackestone. No identifiable grains observed.

PLATE 6

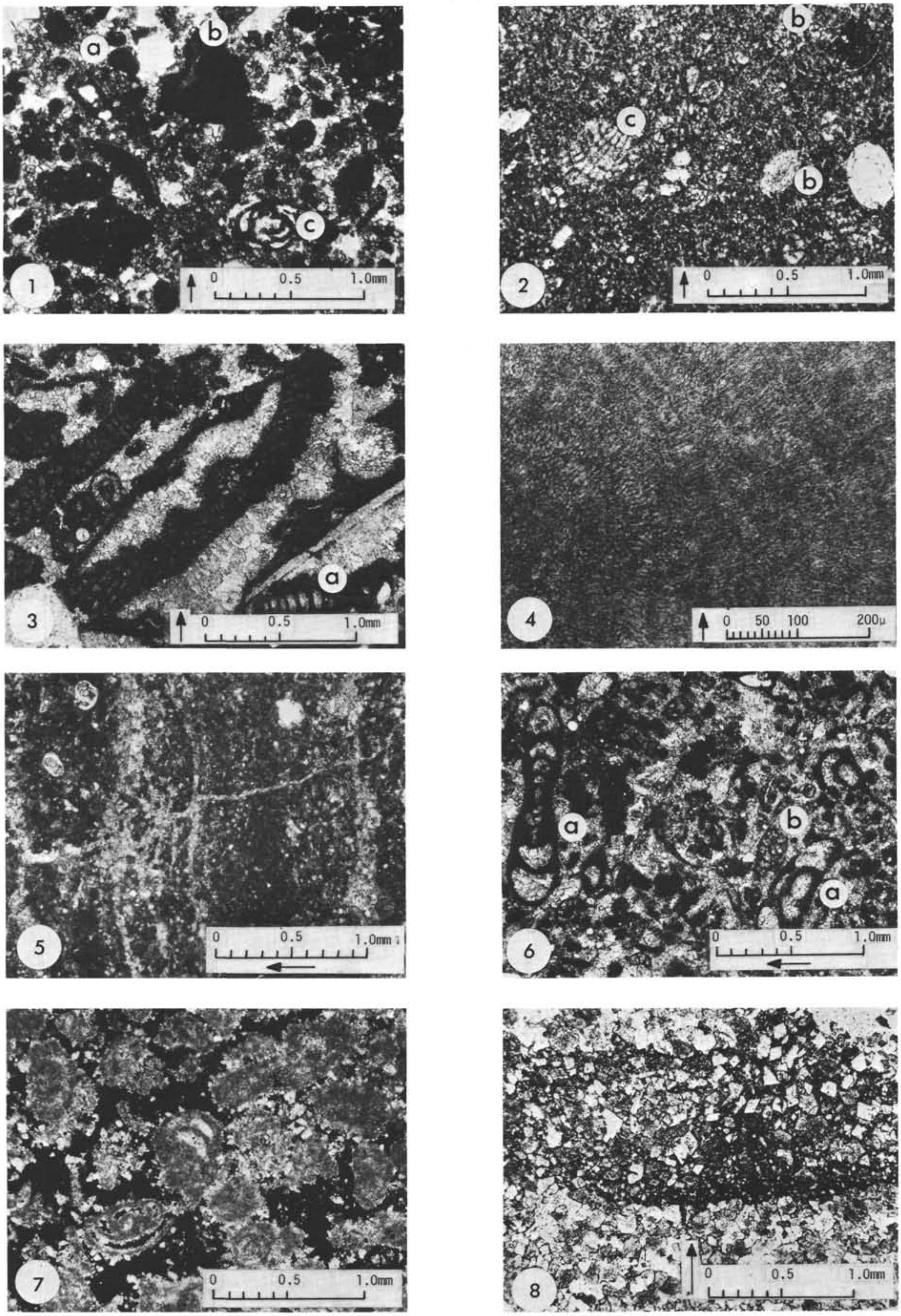
1
a
b
c
0 0.5 1.0mm
2
b
c
b
0 0.5 1.0mm
3
a
0 0.5 1.0mm
4
0 50 100 200µ
5
0 0.5 1.0mm
6
a
b
a
0 0.5 1.0mm
7
0 0.5 1.0mm
8
0 0.5 1.0mm